





This is to certify that the

thesis entitled

# NORMAL ANATOMY OF NAVICULAR BONE AND ITS RELATIONSHIP TO NAVICULAR SYNDROME

presented by

Kimberly Van Wulfen Ernst

has been accepted towards fulfillment of the requirements for

M.S. degree in Anatomy

Major professor

MSU is an Affirmative Action/Equal Opportunity Institution

**O**-7639

# PLACE IN RETURN BOX to remove this checkout from your record. TO AVOID FINES return on or before date due. MAY BE RECALLED with earlier due date if requested.

DATE DUE	DATE DUE	DATE DUE

11/00 c/CIRC/DateDue.p65-p.14

# NORMAL ANATOMY OF NAVICULAR BONE SUSPENSORY LIGAMENTS AND ITS RELATIONSHIP TO NAVICULAR SYNDROME

By

Kimberly Van Wulfen Ernst

# A THESIS

Submitted to
Michigan State University
in partial fulfillment of the requirements
for the degree of

**MASTER OF SCIENCE** 

Department of Anatomy

1999

#### ABSTRACT

# NORMAL ANATOMY OF NAVICULAR BONE SUSPENSORY LIGAMENTS AND ITS RELATIONSHIP TO NAVICULAR SYNDROME

By

# Kimberly Van Wulfen Ernst

The structure of the suspensory ligaments of the navicular bone, the collateral sesamoidean ligament and distal sesamoidean impar ligament (DSIL), has previously been accepted to be that of a typical ligament. Macroscopic and microscopic studies of the region consisting of the DSIL and the deep digital flexor tendon (DDFT) near their common insertion onto the third phalanx, here referred to as the DSIL/DDFT intersection, revealed a structure unlike that of a typical ligament or tendon. Dense, regular connective tissue fibers were interspersed by wide, loose connective tissue septa penetrating through the DSIL and dorsal half of the DDFT. Microscopically, the septa contained many elastic fibers, blood vessels, and nerve fiber bundles, some containing the neuropeptide substance P (SP). Study of the vasculature revealed novel glomus-type arteriovenous complexes (AVC) within the septa. Receptor autoradiography identified receptors for SP on the smaller vasculature and the AVCs. The unusual anatomy of the DSIL/DDFT intersection may explain the effects of intraarticular anesthesia of the distal interphalangeal joint on the sensory nerves to the navicular bone. Also, the unique morphology of this region supports the hypothesis that the DSIL/DDFT intersection may be an important site for the initiation of clinical and pathological features associated with navicular syndrome in equine athletes.

#### **ACKNOWLEDGMENTS**

## Dr. Bowker

With any other advisor, I never would have completed this thesis. Working with Dr. Bowker, I felt I became part of a team. This thesis is only a brief note of a much larger whole and a wealth of ideas. The appropriate words to express thanks can be difficult to find. We developed an outstanding working relationship and a great friendship at the same time. I am honored to have worked with Dr. Bowker and to have learned from him. Someday we may actually have to see how a whiffle ball flies in a wind tunnel.

## Dr. Duke Tanaka

Future veterinary students will never have the opportunity to learn from Dr. Tanaka, but his efforts have not gone unnoticed. His concern for students and their education was clear, as was his sense of humor. Dr. Tanaka was of considerable assistance to me both as a professor of veterinary anatomy and neuroanatomy and a source of advice and encouragement for my master thesis work. He is greatly missed.

# Drs. Mary Rheuben, Steve Schneider, and John Caron

The members of my committee were extremely helpful with their insights, comments, and advice. They were also very flexible and helped to work around my dual degree schedule. Many thanks, and best wishes in your own research!

# TABLE OF CONTENTS

LIST OF TABLES	vi
LIST OF FIGURES	vii
LIST OF ABBREVIATIONS	ix
INTRODUCTION	1
REVIEW OF THE LITERATURE	8
Functional Anatomy	8
Histology	19
Navicular Syndrome	19
Hypotheses for the Pathogenesis of Navicular Syndrome	22
Diagnosis, Treatment, and Prognosis of Navicular Syndrome	26
Neuropeptides	29
Purpose	30
METHODS	32
Macroscopic Anatomy and Histology	32
Elastic Tissue	33
Vasculature	33
Immunochemistry	34
Gold Chloride	35

Autoradiography
RESULTS
Macroscopic Anatomy of the Navicular Suspensory Apparatus
Histology43
Elastic Tissue
SP-like Immunoreactivity
CGRP-like Immunoreactivity
Non-chemically Identified Innervation
The Collateral Sesamoidean Ligament
DISCUSSION91
Histology
Elastic Tissue
Arteriovenous Complexes
Nerves and Neurotransmitters
Function of the DSIL/DDFT Intersection
Forces on the DSIL/DDFT Intersection
Previous Hypotheses
Local Anesthetic
CONCLUSION
APPENDIX
BIBLIOGRAPHY 120
PUBLICATIONS

# LIST OF TABLES

Table	Page
1. Receptor autoradiography data of DSIL/DDFT intersection	116
2. Receptor autoradiography data of hoof wall	117
3. Averages of tables 1 and 2	118
4. Graph of table 3	119

# **LIST OF FIGURES**

Figure Pag	ge
1. Illustration of equine foot, parasagittal section	
2. Parasagittal section of the navicular bone	
3. Bones of the distal horse limb	
4. Normal structural relationships of the bones of the foot when weight bearing 14	
5. Arterial supply to the navicular bone	
6. Macroscopic appearance of the DSIL on coronal section	
7. Normal histology of the DSIL/DDFT intersection (H&E)	
8. Normal histology of the DSIL/DDFT intersection (H&E)	
9. Vasculature of the DSIL/DDFT intersection	
10. Penetrating loose connective tissue septa of the DSIL/DDFT intersection 49	
11-13. Arteriovenous complex	
14. AVC (epithelial - like cells)	
15. Illustration of AVC	
16. Normal histology of the DDFT	
17. Normal histology of the CSL	
18-19. Normal histology of the DSIL and the DSIL/DDFT intersection with van Gieso	nc
stain for elastic tissue	

20.	Normal histology of the DDFT at the flexor cortex of the navicular bone, van G	iieson
	stain	65
21.	Normal histology of the CSL, van Gieson stain	6 <b>7</b>
22-2	23. DSIL with immunochemistry	71
24.	Receptor autoradiography - SP receptor labeling	73
25.	SP receptor labeling around an AVC	76
26.	SP receptor labeling on the dorsal hoof wall	79
27.	CGRP-like immunoreactivity	83
28.	Gold chloride impregnation	86
29.	Photograph of normal CSL	89
30.	Illustration of normal CSL	90
31.	Axon reflex	101
32.	Hypothesis flow chart	107

## LIST OF ABBREVIATIONS

# Abbreviation

AVC = arteriovenous complex

CGRP = calcitonin gene related peptide

CSL = collateral sesamoidean ligament

DDFT = deep digital flexor tendon

DIP = distal interphalangeal (joint)

DSIL = distal sesamoidean impar ligament

DSIL/DDFT intersection = region joining the DSIL and DDFT, including their shared

insertion on P3

EDRF = endothelium derived relaxing factor

NK1 = neurokinin 1 (used in relation to SP; a receptor type)

P1 = first phalanx

P2 = second phalanx

P3 = third phalanx

SP = substance P

#### INTRODUCTION

Navicular disease or syndrome has been the focus of much research attention over the last half century as it presents a major chronic lameness problem of performance horses (Stashak, 1987). Reports discussing the epidemiological factors, clinical and pathological features, diagnosis, and treatment of navicular syndrome (Hickman, 1989; Ostblom *et al.*, 1989a; Ostblom *et al.*, 1989b; Turner, 1991) have given rise to several hypotheses for the etiology of navicular syndrome, including biomechanical causes (Ostblom *et al.*, 1989b; Stashak, 1987; Rooney, 1969; Pool *et al.*, 1989), thrombosis formation (Colles *et al.*, 1977 and 1979), and vascular reorganization resulting from ischemia within the navicular bone (Rijkenhuizen *et al.*, 1989a and 1989b).

The general theme of the several hypotheses regarding a biomechanical etiology involves the deep digital flexor tendon (DDFT) causing compression and/or friction against the flexor surface of the navicular bone, which results in instability in this articulation and changes within the navicular bone. Under certain environmental factors, an increased force or pressure on a bone produces a bony reaction that deposits more bone and orients any bone remodeling so as to add support for the increased forces on the bone (Evans, 1976). Whether the changes in a navicular bone affected by navicular syndrome are regenerative (Pool *et al.*, 1989) or degenerative (Meier, 1996; Rooney, 1969) is disputed. The navicular bone is said to undergo sclerosis (hardening or

induration, Thomas, 1989) and to be degenerating. However, stress placed on a bone normally prevents bony resorption and encourages regeneration, rather than causing degeneration (Carlton *et al.*, 1995). Thus, the plausibility that the lesions observed with navicular syndrome are caused only by the increased forces of the DDFT on the navicular bone is questionable.

Another hypothesis presented for the etiology of navicular syndrome suggests that thrombi block the blood supply to the navicular bone, resulting in ischemic changes in the bone (Colles and Hickman, 1977; Colles, 1979). Thrombi were observed in the distal arteries to the navicular bone, which, compared to the proximal arteries, supply most of the blood to the bone (James *et al.*, 1980; Rijkenhuizen, *et al.*, 1989a). Other researchers have not been successful in finding such thrombi (Pool *et al.*, 1989; Ostblom *et al.*, 1989b; Hickman, 1989; MacGregor, 1989).

Although the previous hypothesis did not confirm the cause of the ischemia, the results of another study were consistent with the idea of ischemia of the navicular bone. Following a compromise in the distal blood supply to the navicular bone, which caused ischemia of the bone, the proximal blood supply was shown to hypertrophy (Rijkenhuizen, et al. 1989b). These authors did not investigate the initial cause of the compromise of the vasculature.

In general terms, the previous hypotheses have all focused on the pathology of the navicular bone as the primary underlying problem of navicular syndrome rather than viewing the radiographic and pathological changes in the navicular bone as secondary to a pathologic condition occurring elsewhere in the foot. These hypotheses have become controversial as each is able to explain only a few of the many features of the syndrome

relating to the clinical lameness, radiographic findings, and pathology. The hypotheses focus on the radiographic and pathological features surrounding only the navicular bone itself. Changes in other structures within the foot, e.g. the distal phalanx (P3), distal sesamoidean impar ligament (DSIL), DDFT, or other parts of the palmar foot, may contribute to known features of navicular syndrome and cannot be fully explained by these previous hypotheses.

We have proposed that the DSIL/DDFT intersection (Figure 1) along with portions of the distal phalanx, rather than only the navicular bone, may be the initiating site for the pathogenic processes of navicular syndrome (Bowker and Van Wulfen, 1996; Van Wulfen and Bowker, 1997). The DSIL/DDFT intersection represents the common region of the DSIL and the DDFT, including their shared insertion on the distal phalanx (Figure 1). With this hypothesis, trauma of sufficient nature to the distal phalanx, the DSIL/DDFT intersection, and the subchondral bones of the joints between the navicular bone and the distal phalanx provides the underlying causal insult to this region. Tearing, bruising, and hemorrhage in the ligamentous tissues caused by stresses during locomotion may result in many clinical features of lameness associated with navicular syndrome and in subsequent tissue inflammatory response within the DSIL/DDFT intersection. Such an inflammatory response produces edema, promotes fibroblast proliferation, and acts with leukocytes and cytokines to alter the metabolism and function of the tissue (Kimball, 1990). This chronic type of inflammatory response may disrupt and alter the blood flow to the navicular bone and caudal foot, eventually producing the reported radiological and pathological features of navicular syndrome. Also, this same inflammatory process may affect the venous drainage of blood from the solar surface of foot, which is critical in Figure 1 Illustration of equine foot, parasagittal section.

Illustration of the median section of a distal horse limb. The orientation of P2 and P3, as well as the navicular bone, is seen in relation to the DSIL and the DSIL/DDFT intersection. The distal extent of the dorsal portion of the DDFT contacts, or "intersects" the DSIL just prior to their insertion on P3. The DSIL/DDFT intersection forms the distal margin of the navicular bursa. The DSIL separates the distal extent of the navicular bursa from the DIP joint.

The squares, labeled a - d for reference, indicate areas from which tissue samples were taken.

H = hoof wall

N = navicular bone

B = navicular bursa

2 = second phalanx

3 =third phalanx

J = distal interphalangeal joint

L = distal sesamoidean impar ligament

T = deep digital flexor tendon

I = DSIL/DDFT intersection

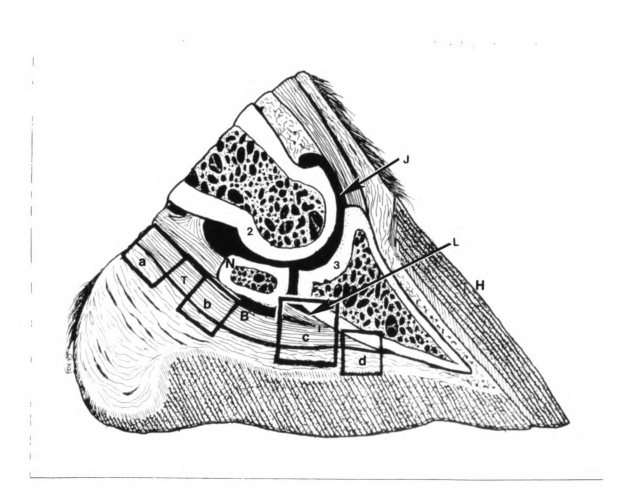


Figure 1 Illustration of equine foot, parasagittal section.

energy dissipation (Bowker, et al., 1998b). One inflammatory mediator likely to have a role in this process is Substance P (SP), known to promote inflammation within injured tissue (Edvinsson, 1993; Kimball, 1990). More recently, the presence of SP in synovial fluid has been shown to increase with naturally occurring osteoarthritis in the horse (Caron, et al., 1992) and with high concentrations of other inflammatory mediators (Kimball, 1990).

Understanding the normal anatomy of the DSIL/DDFT intersection is critically important, not only in regards to beginning to understand the pathogenesis of navicular syndrome, but also in terms of the controversial issue of diffusion of local anesthetics from the synovial cavity of the distal interphalangeal (DIP) joint into the navicular bursa and which structures become desensitized after intraarticular infusion of anesthetic (Bowker *et al.*, 1995a; Dyson and Kidd, 1993; Turner, 1996). While some reports have indicated that no communication between the synovial cavities occurs (Calislar *et al.*, 1969), others have reported that the desensitization effects of the local anesthetics in the DIP joint change temporally (Dyson and Kidd, 1993; Turner, 1996), implying a diffusion of the local anesthetic from the DIP joint into the navicular bursa, as well as into the surrounding tissues of the foot. The actual mechanism of how local anesthetic diffuses through a ligamentous attachment, such as the DSIL, is not known.

Thus, the purpose of this study was to examine in detail the macroscopic and microscopic anatomy of the DSIL and the insertional attachments of the DSIL and DDFT onto the distal phalanx (the DSIL/DDFT intersection). The results will help to determine the morphological features and characteristics of this region, which potentially would be susceptible to traumatic insults, hypothesized to contribute to navicular syndrome. In

addition, the controversial issue of the effects of a local anesthetic injection into the DIP joint and its possible diffusion into the navicular bursa will be addressed in relation to the anatomy of the DSIL/DDFT intersection and in terms of the desensitization of the navicular bone and the caudal foot during a lameness examination.

## REVIEW OF THE LITERATURE

#### Functional Anatomy

The distal sesamoidean impar ligament (i.e. DSIL, impar, distal navicular ligament, distal suspensory ligament) is a short, wide ligament that spans between the distal border of the navicular bone (distal sesamoid) and the flexor surface of the distal or third phalanx (coffin bone, P3) in the equine foot (Figure 1) (Sisson, 1975; Nickel, 1979). As the navicular bone bears a portion of the weight placed on the distal surface of the distal interphalangeal joint, the suspensory ligaments allow the joint to yield slightly on impact to help dissipate the force of concussion (Dyce, 1987). Furthermore, the DSIL must also assist in the weight bearing role of the navicular bone particularly during dorsiflexion of the DIP joint just prior to lift off (Bowker *et al.*, 1998a)(Figure 4). During this dorsiflexion, the DSIL may be under great stress as the navicular bone assumes a substantial weight-bearing load.

The navicular bone, to which the DSIL is attached, is situated in the horse foot just palmar (plantar) to the joint surface between the second and third phalanges (Getty, 1975). Rather than a proximal to distal orientation, the navicular bone's long axis runs in a transverse direction, allowing it to form articular surfaces opposing the second and third (distal) phalanges and a flexor surface opposing the DDFT. The central eminence of the articular surface and the concavities on either side of the eminence of the navicular bone

Figure 2 Parasagittal section of the navicular bone.

This photograph of the navicular bone shows the bone and the important surrounding structures. The distal extent of the navicular bursa can be seen proximal to P3 and not extending completely to P3.

N = navicular bone

B = navicular bursa

2 = second phalanx

3 =third phalanx

J = distal interphalangeal joint

L = distal sesamoidean impar ligament

T = deep digital flexor tendon

I = DSIL/DDFT intersection

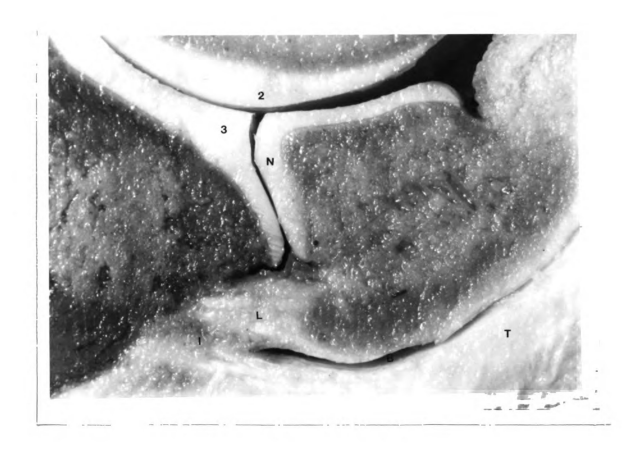


Figure 2 Parasagittal section of the navicular bone.

Figure 3 Bones of the distal horse limb.

This expanded view shows the palmar (plantar) aspect of the bones of the distal

horse limb as viewed in a distal to proximal direction. The insertion of the DSIL/DDFT

intersection is on the solar surface of P3. The x's on the solar surface of P3 indicate the

location of the insertion of the DSIL/DDFT intersection onto P3.

N = navicular bone

2 = second phalanx

3 = third phalanx

J = distal interphalangeal joint

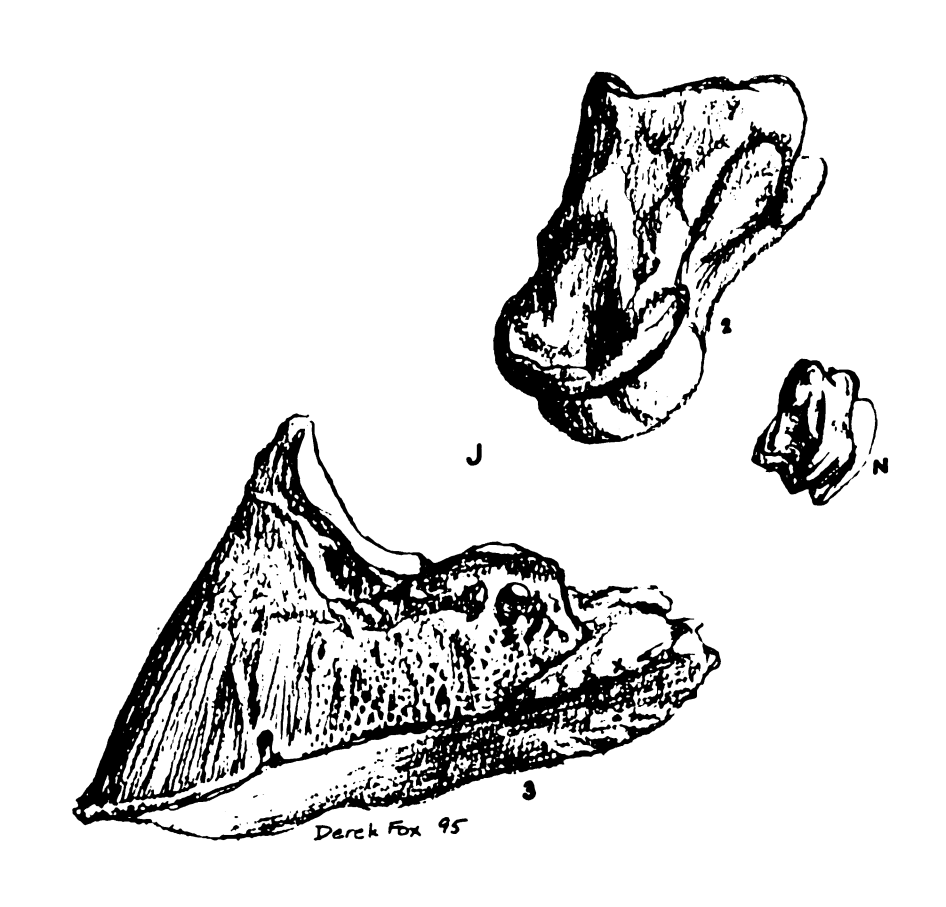


Figure 3 Bones of the distal horse limb.

Figure 4 Normal structural relationships of the bones of the foot when weight bearing.

The force of the weight and momentum of the horse is transferred along the bones of the limbs and their joints. The DIP joint articular surfaces that support the horse include the distal end of P2, the proximal end of P3, and the articular surface of the navicular bone. The navicular bone forms a congruent plane with the articular surface of P3 to support P2. This position of the bones places the suspensory ligaments of the navicular bone under substantial strain from the horse's weight when the foot is in dorsiflexion.

The weight bearing position of the navicular bone is also easily observed with weight bearing radiographs of a horse foot.

H = hoof wall

N = navicular bone

B = navicular bursa

2 = second phalanx

3 =third phalanx

J = distal interphalangeal joint

L = distal sesamoidean impar ligament

T = deep digital flexor tendon

I = DSIL/DDFT intersection



Figure 4 Normal structural relationships of the bones of the foot when weight bearing.

provide for the shape of the distal articular surface of the second phalanx (see Figure 3) (Getty, 1975). The navicular bone is described as providing a constant angle of insertion for the deep digital flexor tendon (DDFT) (Rooney, 1969). This description provides a much different idea for the function of the navicular bone and DSIL as the DSIL cannot apparently yield to absorb loading force during weight bearing without altering its position in relation to P3, thereby changing the insertion angle of the DDFT.

Between the navicular bone and DDFT lies the navicular bursa, which protects the two surfaces from excessive friction and pressure. The distal border of this synovial cavity is inconsistently depicted, shown either to reach the third phalanx (Dyce, 1987) or to end where the DDFT meets the DSIL just proximal to the third phalanx, at the DSIL/DDFT intersection (Stashak, 1987). This inconsistent observation is the result of a misunderstanding of the morphology of the DSIL/DDFT intersection, which forms an interrupted ligament and complicates discernment of the borders of the navicular bursa.

The blood supply to the navicular bone originates from the medial and lateral palmar (plantar) digital arteries (Schummer *et al.*, 1981). Between these two major arteries to the foot, several smaller branches, both proximal and distal to the navicular bone, extend axially to supply the vasculature to the deeper portions of the foot. These smaller branches, the palmar branches of the second (P2) and third phalanges (P3), then give rise to even smaller branches, running in a proximal or distal direction, which then form a network of vessels to supply the navicular bone (James *et al.*, 1980). A variation between the thoracic and pelvic limbs occurs at the level of the distal arterial supply to the bone in that the pelvic limbs have a greater number of arteries entering the distal

border of the navicular bone than do the thoracic limbs (Figure 5) (James et al., 1980). Little is known of the microanatomy of the vasculature of this region.

Figure 5 Arterial supply to the navicular bone.

Adapted from James et al., 1980.

The navicular bone is supplied by proximal and distal arterial sources from the palmar (plantar) digital arteries. These proximal and distal sources then converge and branch, forming secondary and tertiary vessels. From the distal source, which runs through the DSIL, small branches to the navicular bone enter through the nutrient foramina of the distal surface of the bone.

Although the vasculature between limbs is very similar in structure, more distal vessels supplying the navicular bone (within the DSIL) have been shown in the pelvic limb as compared to the thoracic limb (James *et al.*, 1980).

This figure represents a transverse section through the navicular bone, depicting the caudal portion of the foot. The top of the figure is proximal.

A = plantar (palmar) digital arteries, medial and lateral

B = palmar (plantar) arterial branches to P2

C, D, E = primary, secondary, tertiary arteries of proximal network, respectively

F = distal palmar (plantar) branches of P3

G, H = primary and secondary arteries of distal network, respectively

N = navicular bone

\* = more secondary arteries of the distal network (J) are present in the pelvic limbs

# Histology

Precise definitions of the anatomy of the horse foot surrounding the distal navicular bone and the DSIL and this region's potential role in navicular syndrome require consideration of microscopic anatomy as well as macroscopic anatomy.

Tendons and ligaments, commonly known to have tremendous strength, are composed of bundles of dense regular connective tissue with relatively little or scant loose connective and elastic tissue (Dellman, 1993; Mankin and Radin, 1997).

"The great tensile strength of collagen tendons and ligaments is reflected in their structure. They consist of fascicles of parallel collagen fibers. These fascicles are bound together by sparse, loose connective tissue that forms a protective sheath around the blood vessels and nerves of a tendon..."

(Dellman, 1993)

Very little has been reported in the way of histology of the DSIL/DDFT intersection as it is assumed that these structures have the typical histological composition of ligaments and tendons, described above briefly (Dellman, 1993). In addition, the relationship between the blood vessels and nerves of the DSIL and DDFT and their various connective tissue fibers has not been examined.

# Navicular Syndrome

The area of the equine foot near the DSIL is presently of clinical interest due to a devastating lameness condition in horses known as navicular syndrome. Often referred to as navicular disease, the term "syndrome" is used here as it appears likely that this condition may actually be a group of identical or very similar disorders with variations in etiology (complete discussion of which will not be included) (Kobluk *et al.*, 1995; MacGregor, 1989).

A horse with navicular syndrome, most commonly a Quarter horse or Thoroughbred gelding between four and 15 years of age, often has a chronic history of intermittent, shifting-leg, forelimb lameness. The signs usually improve with rest but return once exercise is resumed. As the problem frequently affects both front limbs simultaneously, the horse shows shifting-leg lameness, indicating simply that one foot is more painful and not necessarily that the other is sound. The gait of the horse is usually altered due to the pain experienced when landing on the heel, causing the horse to land on the toe and wear the toe excessively (Stashak, 1987; Kobluk *et al.*, 1995). Such an alteration of the gait is believed to involve the pressure of the DDFT against the flexor surface of the navicular bone (Ostblom *et al.*, 1989a; Pool *et al.*, 1989).

Despite the many proposed hypotheses for the pathogenesis of navicular syndrome, a general description of the disease based on numerous pathological reports is that of a chronic, progressive, degenerative disease affecting the navicular bone, navicular bursa, and flexor tendons (Stashak, 1987; Kobluk *et al.*, 1995; Turner, 1991; Pool *et al.*, 1989a). This description, however, is not universally agreed upon, and new ones are continually being presented. Furthermore, the clinical and radiographic features of navicular syndrome are also highly controversial (Stashak, 1987; Kobluk *et al.*, 1995; Turner, 1991).

The pathologic lesions found in the foot of a horse diagnosed with navicular disease (syndrome) generally include the following changes:

1. Lesions on the flexor surface of the navicular bone and the opposing surface of the DDFT. This region may have a yellow-brown discoloration that is suspected to be due to normal aging processes and thus be simple wear and tear (Stashak, 1987; Kobluk *et al.*, 1995); however, definitive documentation is not available. Eroding or thinning of the fibrocartilage on the flexor surface of the navicular bone may occur, possibly exposing subchondral bone. The subchondral bone then becomes rarefied, dull, granular, and reddened. In addition, the synovial invaginations or vascular channels (often called synovial fossae) along the distal border of the navicular bone may become larger in diameter and number (Stashak, 1987; Kobluk *et al.*, 1995; Hoppner, 1994). These synovial fossae are apparent radiographically and are commonly used as definitive signs of morphological evidence of navicular syndrome.

- 2. In advanced cases, bony erosion of the navicular bone, followed by adhesions between the DDFT and the flexor surface of the navicular bone along the sagittal ridge and the DDFT. Also, osseous metaplasia and sclerotic osteitis of the CSL and DSIL may occur (Stashak, 1987; Kobluk *et al.*, 1995; Pool *et al.*, 1989; Ostblom *et al.*, 1989a; Ostblom *et al.*, 1989b).
- 3. Lesions similar to degenerative joint disease within the navicular bursa. Histopathological lesions have also been reported from feet with navicular disease (syndrome). The fibrocartilage of the navicular bone shows pannus formation with a loss of chondrocytes and ground substance, indicating inflammation and neovascularization. The subchondral bone contains the enlarged vascular channels filled with granulation tissue surrounded by osteoclasts and osteoblasts. New bone formation is indicated by osteoid on the surfaces of the canals. With severe lesions, the DDFT may be involved with adhesions forming between it and the navicular bone (Kobluk *et al.*, 1995; Pool *et al.*, 1989; Ostblom *et al.* 1989a;

Ostblom et al., 1989b). Several reports have documented changes in both the arterial and venous supply of the navicular bone (Colles and Hickman, 1977; Rijkenhuizen et al., 1989b).

The pathological lesions of the navicular bone affected with navicular syndrome have been related to radiographic findings. The list of significant radiographic changes in the navicular bone and nearby structures may vary depending on the stage and clinical presentation of the syndrome, but may include many or most of the following:

- 1. enlarged vascular foramina (also referred to as distal border synovial invaginations)
- 2. cyst formation
- 3. thinning of the flexor cortex (defects)
- 4. marginal osteophytes on the proximal border
- 5. loss of corticomedullary junction
- 6. fracture
- 7. remodeling of the normal shuttle shape of the bone on the lateral margin or distal border
- 8. mineralization of the DDFT.

# Hypotheses for the Pathogenesis of Navicular Syndrome

Hypotheses proposed for the pathogenesis of these pathological changes and the signs associated with navicular syndrome have varied widely, some receiving more attention than others (MacGregor, 1989; Hickman, 1989; Hoppner, 1994).

One hypothesis, which is now often discounted, was proposed by Colles and his colleagues (Colles and Hickman, 1977) after the observation of thrombi in the distal navicular arteries and contends that navicular syndrome is the result of ischemic necrosis of the navicular bone. However, most other investigators have not observed such thrombi even after rather extensive searches in affected feet (Pool *et al.*, 1989; Ostblom *et al.*, 1989a; Ostblom *et al.*, 1989b; Hickman, 1989; MacGregor, 1989). Thus, thrombus formation is unlikely to be the initial or primary cause of this disorder (Stashak, 1987).

Another possible etiology for navicular syndrome is bursitis in the navicular bursa due to conformational problems presumably causing the increased pressure of the DDFT against the navicular bursa and navicular bone (Adams, 1974). The bursitis would then lead to hyperemia and rarification of the bone (Adams, 1974; Stashak, 1987; Kobluk *et al.*, 1995), causing the pain and lameness observed. According to this etiology, horses predisposed are those with poor conformation such as upright pasterns, small feet with a large body, short heels, or long toes.

A rather well known and widely accepted hypothesis for the pathogenesis of navicular syndrome centers on the biomechanical factors that affect this region of the foot. Forces from repeated concussion during locomotion and friction between the navicular bone and DDFT are hypothesized to cause initial physical trauma, resulting in degenerative changes in the bone and tendon (Kobluk *et al.*, 1995). A similar idea, proposed by Pool, Ostblom, and others (Stashak, 1987), is that pressure from the DDFT on the flexor cortex of the navicular bone causes remodeling of the bone with increased bony resorption and formation without ischemia or thrombosis (Stashak, 1987). This is contrary to the observation that bone, when subjected to stress, responds by increasing

new bone formation in an attempt to strengthen and provide the necessary support (Evans, 1976). In addition, an important point that has been overlooked is that pressure by the DDFT against the navicular bone remains fairly constant during most activities and locomotion, regardless of the gait (Schryver, 1978). Consistent with this finding is the fact that the deep digital flexor does not contract during the latter half of the forelimb stride (Konsgaard, 1982). This ensures that the only pressure on the navicular bone from the DDFT is due to the residual tension between fixed attachments of the DDFT, i.e., the inferior check ligament proximally and the insertion onto P3 distally. Thus, more factors must be involved than merely the peak pressure of the DDFT on the navicular bone.

The pathological changes in feet affected with navicular syndrome have also been compared to the changes observed in degenerative joint disease (DJD) (Kobluk *et al.*, 1995). DJD in the distal tarsal joints and pastern results in changes similar to those in the fibrocartilage, flexor cortex, and subchondral spongiosa of the sagittal ridge and the distal border of the flexor surface of the navicular bone (Kobluk *et al.*, 1995). These changes include venous hypertension, increased intraosseous pressure, and fibrosis of the bone marrow stroma of the subchondral cancellous bone (Kobluk *et al.*, 1995). This comparison to DJD focuses mainly on the navicular bone as the primary focal pathological site.

In a brief report by Wintzer (Wintzer and Schlarman, 1971), changes in the DSIL were reported to occur with navicular syndrome, suggesting that the pain in this disorder may originate at this site. Unfortunately, this report is not widely known or accepted as it was thought to have only a minor role in contributing to the pathogenesis of navicular syndrome.

Relatively recent work on the pathogenesis of navicular syndrome has been performed by Rijkenhuizen and her colleagues (Rijkenhuizen et al., 1989b). Following extensive studies of the normal arterial supply in the fetus, foal (Rijkenhuizen et al., 1989c), and adult horse (Rijkenhuizen et al., 1989a), the blood supply to the navicular bone of horses with clinical and/or radiographic signs of navicular syndrome was examined and was found to be altered from the normal state. The diameter of the vessels of the arterial supply entering the distal portion of the navicular bone was significantly reduced, while the diameter of those entering the proximal and abaxial portions of the bone was increased. These researchers concluded that the proximal, medial, and lateral blood supply compensated for the compromise of the distal supply. In addition, the arteriosclerosis that was observed in and around the nutrient foramina of the distal navicular bone suggested that the origin of the vascular changes was either inside or very near the distal portion of the navicular bone. However, an experimental attempt to reproduce the signs of navicular syndrome by resecting the medial and lateral palmar digital arteries was not successful as permanent clinical changes were not produced (Rijkenhuizen et al., 1989d). This study concluded that the clinical, radiological, and histological changes observed in a horse with navicular syndrome may be due to a vascular compromise in addition to other factors that contribute to the development of the features associated with navicular syndrome. These additional factors may include environment, conformation, and breed, which are likely to be critical in the pathogenesis of this disease.

In this same experiment (Rijkenhuizen et al., 1989d), the arterial branches to the distal navicular bone were occluded, which resulted in radiographic changes consistent

with navicular syndrome such as increased bone remodeling in the distal part of the navicular bone. The authors concluded that a reduced blood supply entering the distal portion of the navicular bone may be important in the pathogenesis of navicular syndrome. Brief note was taken of the DSIL to mention that within it, no ischemic or necrotic lesions were found (Rijkenhuizen *et al.*, 1989e). However, clinical features of the disease were not associated with this experimental model.

Thus, the pathogenesis of navicular syndrome appears to be very controversial (Hoppner, 1994), and no unifying concept or hypothesis has been formulated that may explain most all of the clinical, radiographic, and post mortem features of the disease.

## Diagnosis, Treatment, and Prognosis of Navicular Syndrome

The diagnosis of navicular syndrome has become complex and controversial. First of all, without a confirmed and understood pathogenesis, it is difficult to define the exact nature of the condition and the cause of the lameness. Secondly, and also related to the ambiguity of the pathogenesis, a successful treatment protocol has not been established, and no "cure" is available. Horse owners regard navicular syndrome as a very serious diagnosis as it is not completely reversible, will require long-term management, and may negatively affect the performance of the horse, possibly ending an athletic career. Thus, clinicians are frequently reluctant to diagnose navicular syndrome without meeting rather stringent qualifications, including the presence of radiographic changes in the navicular bone. Other clinicians may diagnose clinical navicular syndrome based on the clinical features alone.

Suggestive clinical signs in the patient's history and physical examination are the first keys to the diagnosis of navicular syndrome. Owners or trainers complain of a chronic lameness condition that tends to alternate between the front limbs, improves with rest, and recurs with resumed exercise and work. The gait of these horses is usually described as short and choppy as the horse tries to land on the toe of the foot, and the horse may stumble or trip at times. When standing, the horse may extend the leg of the more painful foot or place both feet forward (Stashak, 1987; Kobluk *et al.*, 1995; MacGregor, 1989).

An important part of the physical examination is observation of pain elicited with the use of hoof testers. Pain over the central third of the frog is a common finding (Stashak, 1987); however, this must be carefully interpreted as it may indicate other causes of pain in the caudal portion of the foot (Kobluk *et al.*, 1995). In addition, a negative response to hoof testers (no pain elicited) does not necessarily indicate that lesions are not present, and any findings should be compared to those of the opposite foot.

To further locate the origin of the pain, several other tests can be performed. Flexion tests of the joints of the distal limb may isolate the pain to the DIP joint. Desensitizing the medial and lateral palmar digital nerves will improve the lameness in 90% or more of the horses affected with navicular syndrome (Kobluk *et al.*, 1995). Finally, injection of local anesthetics into the navicular bursa should result in significant improvement of the lameness (Stashak, 1987; Kobluk *et al.*, 1995; MacGregor, 1989). However, local anesthetic injections into the DIP joint may also result in improvement, and these effects remain controversial in terms of the diagnosis of navicular syndrome. Most clinicians have believed that local anesthetic solution achieved its effect by reaching

the flexor cortical surface of the navicular bone, which forms the dorsal border of the navicular bursa (Dyson et al., 1993). As a result, these findings raised questions concerning diffusion of local anesthetic and possible synovial cavity communication. With all of these tests, however, it is crucial to note that they are not entirely specific for pain originating from the navicular bone or adjacent structures, but only that the painful condition is present in the caudal foot (i.e. palmar foot pain).

Some researchers and clinicians hold the opinion that the diagnosis of navicular syndrome cannot be made or confirmed without radiographic findings consistent with the disorder, while others are adamant that clinical pain in the region is consistent with such a diagnosis. This controversy may have evolved from the poor prognosis associated with the syndrome and the impact of the syndrome on the athletic performance of the horse. Although some clinicians rely on observing the radiographic changes prior to making the diagnosis of navicular syndrome, many of these observed changes in the bone will not be seen radiographically until nearly 40% of the density of the bone is lost (Hickman, 1989). The radiographic signs were listed previously in the explanation of navicular syndrome.

Attempts to manage a horse affected by navicular syndrome may involve several types of treatment. Stall rest is usually recommended initially. Medical management has been quite varied, but it often includes nonsteroidal anti-inflammatory drugs. Although difficult to maintain and regulate, anticoagulant therapy, in line with Colles's hypothesis (Stashak, 1987), has been reported to have some success. Also targeting the vasculature, isoxuprine hydrochloride, an anti-sympathomimetic drug (peripheral vasodilator), has been given to dilate peripheral arteries (Stashak, 1987). Intrabursal (navicular bursa) injections of steroids are also reported (Stashak, 1987). Generally, the affected feet are

trimmed to raise the heel and roll the toe as well as to align the hoof-pastern axis in an attempt to relieve the pressure of the DDFT on the navicular bone. Surgical treatments include cryogesia of the palmar digital nerves (which supply the caudal portion of the foot), desmotomy of the CSL, inferior check desmotomy, and even as drastic a procedure as palmar digital neurectomy, which has several severe complications possible (Stashak, 1987; Kobluk *et al.*, 1995). Many other treatment options are also available and have been utilized in the treatment of navicular syndrome.

## Neuropeptides

Factors that contribute to the etiology of disease include immunoglobulins, vasoactive amines (histamine, serotonin), proteins (lymphokines, interferons, kinins), and neuropeptides (Slauson, 1990). Of these, the neuropeptides are present both in sensory nerves and in leukocytes (mast cells) and have been shown to have a significant role in promoting inflammatory processes (Kobluk *et al.*, 1995; Kimball, 1990). The effects of these neuropeptides include vasodilation, edema formation, chemoattraction of white blood cells, and facilitation of the release of intracellular contents of mast cells (Kimball, 1990). In addition, the presence of substance P (SP) and calcitonin-gene-related peptide (CGRP), both neuropeptides, in sensory nerves and the relationship of these nerves to blood vessels imply an interaction between the immune, vascular, and sensory nervous systems. The neuropeptides that are most studied are the tachykinins, including substance P (SP), neurokinin A (NKA), and neuropeptide K. These are peptides that all have a common C-terminal amino acid sequence: Phe-X-Gly-Leu-Met-NH2.

Substance P is an eleven amino acid peptide that may be present in the sensory nerve fibers supplying most, if not all, of the blood vessels in the body (Edvinsson, 1993). This peptide is reported as having many functions, including peripheral vasodilation, venoconstriction, promotion of the release of prostacyclin, and an increase in capillary permeability. Although other cell types may also be affected, SP is known to act on arterial and capillary endothelia and arterial and venous smooth muscle fibers. SP may be important in neurogenic inflammatory reactions in tissues through neurokinin-1 (NK1) receptor types that mediate the release of endothelium-derived relaxing factor (EDRF), histamine, and prostaglandins (Edvinsson, 1993). SP may maintain chronic inflammation by its promotion of the production of interleukin-1 (Edvinsson, 1993; Kimball, 1990).

A second neuropeptide, CGRP, is a 37 amino acid peptide present in sensory nerves that potentiates the tissue response to tachykinins such as SP and is suspected to have a sensory function (Edvinsson, 1993). In some species, immunoreactivity studies have shown SP and CGRP to coexist in a population of sensory ganglion cells (Edvinsson, 1993; Kimball, 1990). More specifically, CGRP and SP are found in the same large granular vesicles, called peptidergic-type (p-type) vesicles. These p-type vesicles have been observed within mitochondria-rich nerve terminals, presumed to be mechanoreceptors, supplying a variety of blood vessels (Edvinsson, 1993; Kimball, 1990). Their possible roles in the horse and in navicular syndrome are unknown.

### Purpose

After reviewing previous studies and reports, it is evident that much is known about the clinical signs and diagnosis, including radiographic findings, of navicular

syndrome (Stashak, 1987; Turner, 1991). Despite this knowledge, the results of treatments for navicular syndrome, some previously mentioned, are varied and often unsatisfactory, which is likely due to our lack of understanding of the pathogenesis of the syndrome. Following the examination of feet of normal horses and horses afflicted with both the clinical and radiographic changes associated with navicular syndrome, we have formulated the hypothesis that the DSIL/DDFT intersection may be an important and critical site in this disease process (Bowker and Van Wulfen, 1996; Van Wulfen and Bowker, 1997). Thus, the goals of this study were (1) to examine in normal horses the DSIL and its intersection with the DDFT that are structures in anatomical proximity to the diseased areas in navicular syndrome, and (2) to determine if the morphology of this region may contribute to the understanding of the pathogenesis of navicular syndrome. These goals are based on the premise that the composition of the DSIL/DDFT intersection may be susceptible to injury and may be able to provide an inflammatory response to that injury, thereby initiating the pathogenesis of navicular syndrome.

#### **METHODS**

## Macroscopic Anatomy and Histology

Equine feet (n=30) were obtained from the Veterinary Teaching Hospital at Michigan State University from horses of various breeds including Quarter Horse, Arabian, Standardbred, Appaloosa, and Thoroughbred. The horses ranged in age from less than one year to 30 years, were clinically sound, and had no recent history of lameness. The forelimbs were removed just distal to the carpal or tarsal joint. In one phase of the experiments, feet were cut on a band saw either parasagittally or coronally into 0.5-0.7 cm sections and the sections were examined macroscopically for visible anatomical signs of pathology of the navicular bone and its ligaments. No horses with a known history of lameness or evidence of pathology within their feet, such as adhesions between the navicular bone and DDFT, were included in this portion of the study. The tissue samples were then placed in a 10% formalin solution buffered with sodium phosphate (pH 7.2-7.4) for two days to one week. The DSIL/DDFT intersection, as well as tissue samples from the CSL, the DDFT at the flexor surface of the navicular bone, and the DDFT at the level of the CSL, were isolated and prepared for histological examination. These tissues were then sectioned on a freezing microtome at 90 µm, and the sections were mounted on glass slides, stained with eosin Y and methylene blue, and coverslipped before they were examined under a microscope.

#### Elastic Tissue

In addition to routine histology, elastic tissue was identified using tissue samples from the DSIL/DDFT intersection, the DDFT, and the CSL that were fixed and processed for paraffin embedding. Once mounted onto the slides, the sections were stained for elastic fibers with the van Gieson stain prior to examination under the microscope. Tissue sections from the aorta served as control tissues for staining of elastic fibers. The tissue preparation procedure was performed by the Animal Health Diagnostic Laboratory at Michigan State University.

#### Vasculature

To observe the vascular patterns of these tissues, ten feet were perfused with India ink by first flushing the vasculature with 300 to 500cc of saline. Next, the feet were infused with 120cc of a solution of 30% India ink and 5% gelatin in 0.1 M sodium phosphate buffer (pH 7.4) via the medial palmar artery (7 feet) or the dorsal metatarsal artery (3 feet) with a 60 cc handheld syringe. Prior to infusing the last 30-40 ml of the India ink solution, the vessels (veins) were ligated with hemostats to ensure adequate and complete filling of the foot vasculature. All vessels were then tied off at the proximal metacarpus (or metatarsus) to prevent loss of the perfusate, and the limbs were placed upright in a freezer at minus 10-15°C for several days to one week. The frozen limbs were sectioned (0.5-0.7cm) parasagittally on a band saw and placed in buffered formalin. After 24 hours, the DSIL/DDFT intersection was dissected out and placed into a sequential series of gelatin solutions, ranging in concentration from 10% to 25%, at 36°C for 12-24 hours each. The tissues were subsequently embedded in 25% gelatin and

chilled at 4°C, after which the tissue was suspended within a gelatin block that was then placed in a 5% formalin solution for 24 hours in order to solidify and fix the gelatin. The gelatin blocks were sectioned on a freezing microtome at 90 µm, and the sections were collected serially. They were dipped into a sodium acetate buffer mounting solution that consisted of 100 ml 0.2 M acetic acid, 1.64 g sodium acetate, 250 ml 100% ethanol, and 1500 ml distilled water. The sections were mounted on electrically-charged Fischer Superfrost Plus Microscope slides and allowed to dry overnight. Finally, they were stained using eosin Y and methylene blue and coverslipped before being examined under the microscope.

### *Immunochemistry*

Tissue samples from the DSIL/DDFT intersection were fixed in 10% buffered formalin for 24 hours and prepared for immunochemistry using a rabbit polyclonal antisera raised to SP. After tissues were cut on a freezing microtome at 60 μm, sections were rinsed, processed routinely as for immunochemistry, and then incubated for 24-48 hours at room temperature in primary antisera directed against SP. Following this incubation, the sections were rinsed in 1% normal goat serum (4°C) in 0.1M sodium phosphate (pH 7.4), incubated in secondary biotinylated antibody (biotinylated goat antirabbit IgG) (Vectastain) for 3-4 hours, rinsed again, and then placed in an avidin-biotinylated peroxidase complex (Vectastain) for 3-4 hours. The tissues were then rinsed in 0.1M sodium phosphate buffer followed by 0.1M sodium acetate buffer prior to reacting them using diaminobenzidine HCL and 1-2% nickel ammonium sulfate. All rinses and control solutions were at room temperature unless otherwise noted. Controls

for immunochemistry experiments to document specific and nonspecific binding were performed by adding a ten-fold excess of the peptide substance P to the first incubation solution with the primary antisera raised to substance P and by omitting the primary antiserum from this solution.

Additional immunochemistry experiments were performed, substituting primary antisera directed against CGRP for SP antisera.

#### Gold Chloride

From unfixed, fresh feet, tissue samples of the DSIL/DDFT intersection were obtained to be impregnated with gold chloride, according to the technique of Zimny (Zimny, 1985) that identifies both myelinated and unmyelinated nerve fibers. Blocks of tissue less than 1 cm in thickness were incubated in a series of solutions containing fresh-squeezed lemon juice, 1% gold chloride, and 10% formic acid solution. After impregnation, the sections were cut on a freezing microtome at 90 µm, mounted on glass slides, and passed through a series of solutions of increasing alcohol concentrations and into xylene prior to being coverslipped. The gold impregnated tissue sections did not require counterstaining.

## Autoradiography

Receptor autoradiography was performed on fresh, unfixed tissue following the technique of Mantyh (Mantyh et al., 1989). Collected tissues, consisting of both the DSIL/DDFT intersection and the dermis and inner portion of the dorsal hoof wall containing vascular samples, were obtained within 10-15 minutes of euthanasia and

rapidly frozen using dry ice. The DSIL/DDFT intersection and dermis were sectioned on a cryostat at 20 μm, thaw-mounted onto glass slides, placed into a slide box, and returned to a low temperature freezer (minus 80°C) where they were stored until processed for receptor autoradiography. All slides were placed first into a pre-incubation solution, which consisted of 50 mmol Tris-HCl and 0.005% v/v polyethylenimine (pH 7.4), for 20 minutes. One slide of three adjacent sections was then placed in one of the following three incubation solutions for one hour in a coplin jar at room temperature (21-22°C):

Solution 1: 20 pmol/L I-BHSP (Iodine 125-Bolton-Hunter SP), 50 mmol/L Tris-HCl, 3 mmol/L MnCl<sub>2</sub>, 200 mg/L bovine serum albumin, 2 mg/L chymostatin, 4 mg/L leupeptin, 40 mg/L bacitracin (pH 7.4). I-BHSP was supplied by the Amersham Corporation, 2636 South Clearbrook Drive, Arlington Heights, Illinois, 60005.

Solution 2: solution 1 plus 1 µmol/L unlabeled substance P (SP)<sup>3</sup>.

Solution 3: solution 1 plus 50 nmol/L specific NK1 receptor agonist [sar<sup>9</sup>, Met (O2)<sup>11</sup>]-substance P<sup>4</sup>.

Samples of 10 µl taken from each of the three incubation solutions prior to and at the conclusion of the experiment were measured for radioactivity by scintigraphy (Hood *et al.*, 1978). No significant difference between corresponding samples was found.

The slides were removed from the incubation solutions and passed through a series of wash solutions prior to being rapidly rinsed in distilled water. The slides were dried quickly with cold compressed air passed over desiccant and stored overnight at minus 80°C.

To visualize the radioactivity of the sections, the slides were apposed to Kodak X-OMAT AR film in a radiographic cassette equipped with two Dupont Cronex Hi-Plus intensifying screens. A microscale strip of I<sup>125</sup> corresponding to the manufacturing date of the I<sup>125</sup> - SP was also apposed to the film. After 2-7 days, the film was developed in an automatic processor. All films from an experiment were processed on the same day.

The slides of the tissue sections were counterstained with methylene blue and eosin Y and coverslipped. The autoradiographic film was cut and positioned onto glass slides corresponding to the histological slides identified by tissue, experiment, and date. The two slides could then be compared to match the histological components of the tissue with the silver grain retention on the radiographic film. A Leitz microscope equipped with a video camera projected the images to a monitor, the final magnification being 83x.

Quantitative microdensitometry of the autoradiographic film was performed by a Bioquant Meg IV system (version 2.6.92) that, using the microscale of known radioactive levels, determined the radioactivity of the tissue sections.

Four areas of the slides were quantitated:

- 1. the slide itself, with no tissue (background)
- 2. tissue with no visual evidence of radioactive binding (plain tissue)
- 3. nonspecific binding sites of radiolabeled SP, such as cut edges of tissue that showed binding on all tissue sections irrespective of incubation solution (nonspecific binding)
- 4. specific radiolabeled SP sites on tissue (specific binding).

The tissue to be quantitated was identified with the microscope, the coordinates were recorded, and the portion of interest was outlined on the video image. The outline

was saved and was then overlaid onto the image of the autoradiographic film slide over the corresponding portion of interest. The Bioquant system measured surface area and optic density for each outlined region from each slide and each of the four regions above listed. Calculations averaged the density of the areas and resulted in a density per unit area.

Ten microscales from the manufacturer were of known radioactivity at the time of shipment with the I-BHSP, and by following a radioactive decay chart, the radioactivity level was calculated using the following dates: the day the experiment was performed, the day the film was exposed, and the day the film was developed. The radioactivity of each microscale was entered into the standardization table that translated the optic density measured into radioactive values.

Eight horses were evaluated, using three tissue sections of each as previously described. From each slide, four measurements from each of the four regions listed above were taken, which were then averaged. The data on SP receptor localization was collected and analyzed.

#### **RESULTS**

Previous anatomical descriptions of the distal suspensory ligament of the navicular bone (DSIL, or distal sesamoidean impar ligament) and the dorsal DDFT at the intersection of the two structures distally near P3 have been limited to macroscopic examination, primarily in the parasagittal plane (Nickel, 1979). However, our detailed examinations have revealed that the DSIL/DDFT intersection appears to be very unique and complex in its tissue composition, both on macroscopic and microscopic evaluation, in comparison to other ligamentous and tendinous attachments in the distal horse limb.

## Macroscopic Anatomy of the Navicular Suspensory Apparatus

A foot was cut parasagittally, allowing manipulation of the interior structures surrounding the navicular bursa. Displacement of the DDFT palmarly from the navicular bone permitted visualization of the distal aspect of the navicular bursa from an internal perspective. The DSIL and the dorsal surface of the DDFT, as they joined to form the DSIL/DDFT intersection near their insertion onto P3, also formed the distal extent of the navicular bursa. From this internal viewpoint, thin strands of connective tissue were seen extending between the DSIL dorsally and the DDFT palmarly, forming sheets of dense connective tissue separated by distal evaginations of the synovial cavity. The connective

tissue sheets between the DSIL and DDFT preclude the full extension of the navicular bursa to the bony surface of the distal phalanx.

The DSIL and DSIL/DDFT intersection, viewed from the inside of the distal interphalangeal joint on a coronal section, were observed to consist of distinct, nearly parallel bands of collagen fibers with loose connective tissue (1-3 mm in width) between these fibrous bands. This arrangement of the loose connective tissue formed septa (separating the dense connective tissue) that extended from the dorsal surface of the DSIL and penetrated through the dorsal half (approximately) of the DDFT (Figure 6). The loose connective tissue appeared to contain extensive microvasculature due to the red coloration of the tissue. In addition, the glistening white strands appeared to have an elastic component. The DSIL with its penetrating septa into the DDFT and the common insertion of the DSIL and DDFT onto the distal phalanx collectively formed the region referred to as the DSIL/DDFT intersection.

Figure 6 Macroscopic appearance of the DSIL on coronal section.

This horse foot was cut coronally at the level of the DSIL and DSIL/DDFT

intersection. The light gray, nearly parallel bands of tissue were the dense connective

tissue collagen fibers of the DSIL/DDFT intersection. Between these fibers were the

loose connective tissue septa, which appeared darker gray and less rigid in consistency.

The loose connective tissue septa were found throughout the DSIL/DDFT intersection

and, by their interconnections around the dense connective tissue fibers, spanned from the

DIP joint into the navicular bursa.

D = dense connective tissue collagen fibers

S = loose connective tissue septa



Figure 6 Macroscopic appearance of the DSIL on coronal section.

#### Histology

Histological sections allowed for a more detailed evaluation of the morphology of the DSIL/DDFT intersection, confirming that the structures seen macroscopically consisted of dense and loose connective tissues with extensive microvascular and neural networks. Between the dense connective tissue bands were wide areas of loose connective tissue that contained numerous small blood vessels and nerves (Figures 7,8,9). These loose connective tissue septa were seen throughout all regions of the DSIL/DDFT intersection from dorsal to ventral, appearing to be continuous through the ligament and tendon (Figure 10).

The blood vessels present in the loose connective tissue septa were best demonstrated with tissues from the India ink infused feet. When histological sections from these feet were examined, they revealed the presence of many small blood vessels (arterioles, venules, and capillaries) as well as novel vascular structures within the loose connective tissue septa. These novel vascular structures, which resembled arteriovenous complexes (AVCs) in their appearance, could be followed through three to eight serial sections at 90 um as the India ink made the individual vessels more evident. In series of three to six consecutive sections, a column of India ink was observed to pass from one larger, thick-walled vessel into a tortuous, coiled capillary network prior to entering a larger, thin-walled vessel (Figures 11, 12, 13). This capillary network was not observed to branch out to supply the surrounding tissue but to form a glomus-type structure that was surrounded by epithelial-like cells (Figures 14, 15). These complexes ranged in size from 500 to 1400 µm and were seen only in the DSIL/DDFT intersection and not in the DDFT or CSL sections examined (Figures 16, 17).

Figures 7, 8 Normal histology of the DSIL/DDFT intersection with routine H&E stain.

Fiber bundles were evident in the dense connective tissue portions of the

DSIL/DDFT intersection. Large areas of loose connective tissue, which appeared less

rigid in structure and contained the many blood vessels, separated bundles of fibers. See

inset c on figure 1 for the origin of the tissue sample.

D = dense connective tissue

S = septa (loose connective tissue)

V = blood vessels

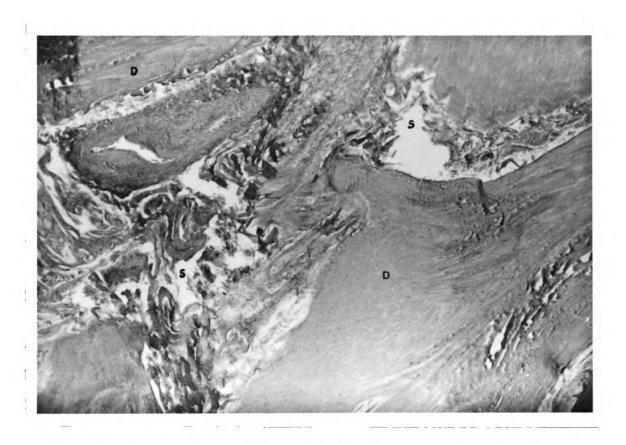


Figure 7 Normal histology of the DSIL/DDFT intersection with routine H&E stain.

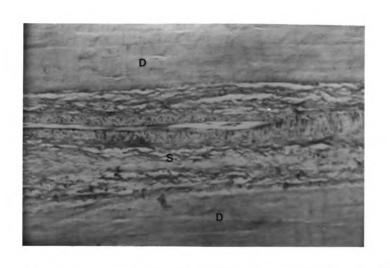
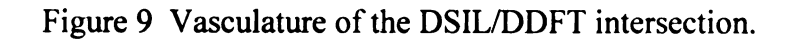


Figure 8 Normal histology of the DSIL/DDFT intersection with routine H&E stain.



The many small vessels and groups of vessels (possibly AVCs) were seen within the loose connective tissue of the DSIL/DDFT intersection.

D = dense connective tissue fibers

S = loose connective tissue septa

V = blood vessels

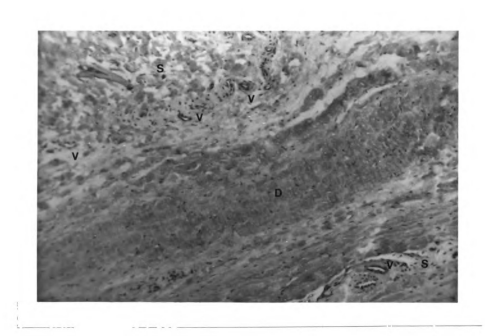


Figure 9 Vasculature of the DSIL/DDFT intersection.

Figure 10 Penetrating loose connective tissue septa of the DSIL/DDFT intersection.

The DSIL is located at the top of the photographs and the dorsal portion of the

DDFT at the bottom. The loose connective tissue running between is a portion of one of

the septa. These penetrating loose connective tissue structures were found throughout the

DSIL/DDFT intersection. The adjacent septa were interconnected around fiber bundles,

forming a continuous network through the DSIL/DDFT intersection from the DIP joint

dorsally to the navicular bursa palmarly (plantarly). See inset c on figure 1 for the origin

of the tissue sample.

L = DSIL

T = DDFT

S = loose connective tissue septa



Figure 10 Penetrating loose connective tissue septa of the DSIL/DDFT intersection.

Figures 11, 12, and 13 Arteriovenous complex (AVC).

These three photographs were taken from three serial slides of coronal sections of

the DSIL/DDFT intersection. In the first section (Figure 11), the AVC began with a

larger vessel, which in the photograph appears as the large, black, circular structure due to

the India ink. From the larger vessel, several smaller vessels branched off and gave rise

to a glomus-type structure of tortuous capillaries that appeared to twist around one

another but did not radiate into the surrounding tissue (Figure 12). These tortuous

capillaries then emptied into a larger collecting vessel (Figure 13). Similar vascular

structures were found to extend through as many as 12 adjacent sections, each section

being 90 µm.

A = supplying vessel

C = tortuous capillary network

V = collecting vessel

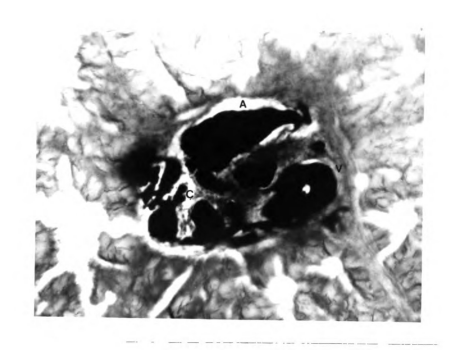


Figure 11 Arteriovenous complex (AVC).

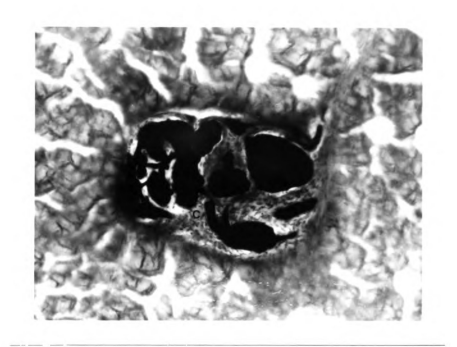


Figure 12 Arteriovenous complex (AVC).



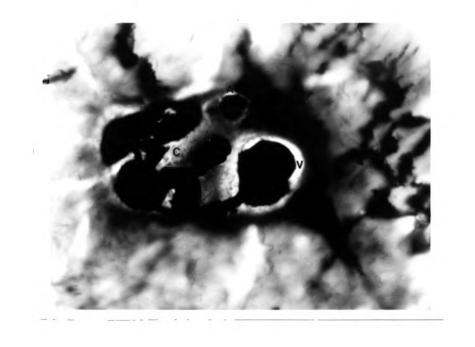


Figure 13 Arteriovenous complex (AVC).

Figure 14 AVC (epithelial-like cells).

This photograph of an AVC was taken at a lower magnification as compared to figures 11 - 13 to improve the visibility of the epithelial-like cells that surround the AVCs within the loose connective tissue septa.

E = epithelial-like cells

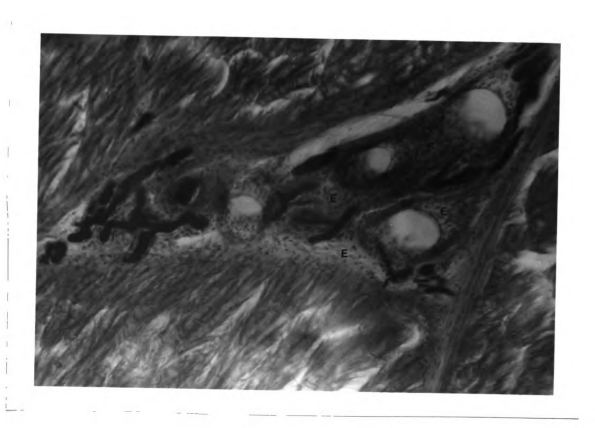


Figure 14 AVC (epithelial-like cells).

# Figure 15 Illustration of AVC.

This figure was constructed from four serial sections of an AVC in the DSIL/DDFT intersection. Again, the large supplying vessel gave off several capillaries, forming the glomus structure. The capillaries then entered a collecting vessel.

A = supplying vessel

C = capillary network

V = collecting vein

E = epithelial-like cells

D = dense connective tissue

S = loose connective tissue septa

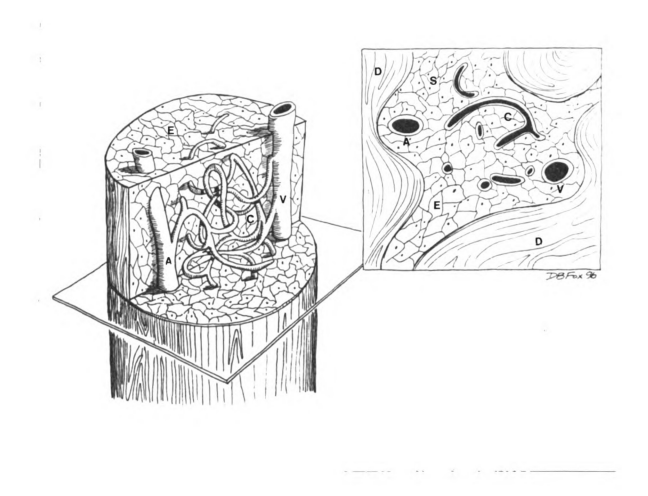


Figure 15 Illustration of AVC.

Figure 16 Normal histology of the DDFT.

Sections from the DDFT, obtained from regions proximal to the DSIL/DDFT intersection (see boxes a and b in figure 1), were found to consist almost entirely of dense regular connective tissue. The unique nature of the composition of the DSIL/DDFT intersection (see figures 7, 8) becomes more evident in comparison to other tendons and ligaments of the horse foot.

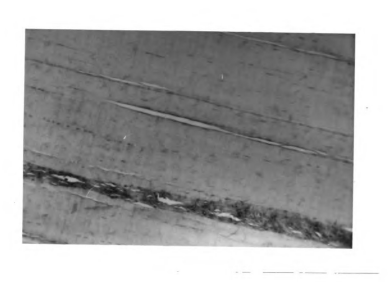


Figure 16 Normal histology of the DDFT.

Figure 17 Normal histology of the CSL.

The histology of the CSL was found to be that of a typical ligament or tendon, consisting of regular, dense connective tissue with only sparse loose connective tissue surrounding a few vessels.

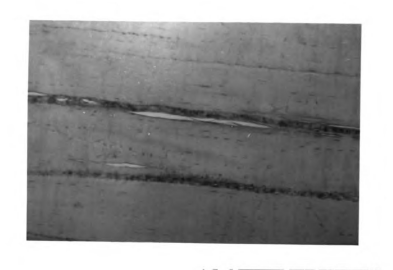


Figure 17 Normal histology of the CSL.

## Elastic tissue

The composition of the connective tissue of the DSIL/DDFT intersection was evaluated more closely with the van Gieson elastic stain. The approximate density of elastic fibers in the DSIL and DSIL/DDFT intersection was compared to that in the DDFT and other ligaments and tendons within the equine digit. Elastic fibers are normally present in ligaments, but the DSIL/DDFT intersection appears to contain a relatively large number of elastic fibers in comparison to other ligaments within the digit (Figures 18, 19). These elastic fibers extended into the dorsal half of the DDFT and were much more abundant than in more proximal sections of the DDFT (Figure 20) and of the CSL (Figure 21). The DDFT contained little to no elastic tissue as compared to the DSIL. In addition, other adjacent ligaments (straight sesamoidean ligament of the DIP joint) contained considerably less elastic tissue than the DSIL and DSIL/DDFT intersection. Such a comparative assessment could be determined as the tissues were stained simultaneously, using the elastic composition of the aorta as the control tissue.

Figures 18, 19 Normal histology of the DSIL and the DSIL/DDFT intersection with van Gieson stain for elastic tissue.

The black lines and dots through the tissue are elastic fibers, which were located within the loose connective tissue septa. The concentration of these fibers was greater than would be expected in a normal ligament.

S = loose connective tissue septa

D = dense connective tissue fibers

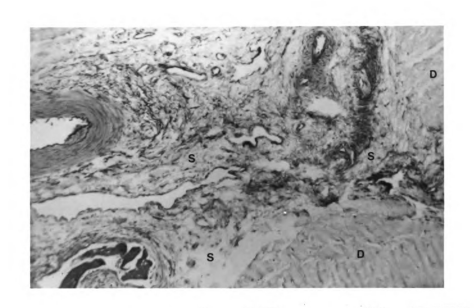


Figure 18 Normal histology of the DSIL and the DSIL/DDFT intersection with van Gieson stain for elastic tissue.



Figure 19 Normal histology of the DSIL and the DSIL/DDFT intersection with van Gieson stain for elastic tissue.

Figure 20 Normal histology of the DDFT at the flexor cortex of the navicular bone, van Gieson stain.

The DDFT was examined for comparison and was found to have the relative density of elastic tissue as would be expected of a tendon or ligament. To appreciate the contrast, please compare this figure to figures 18 and 19 of the DSIL, demonstrating the relative abundance of elastic tissue fibers. See inset b on figure 1 for origin of the tissue sample.

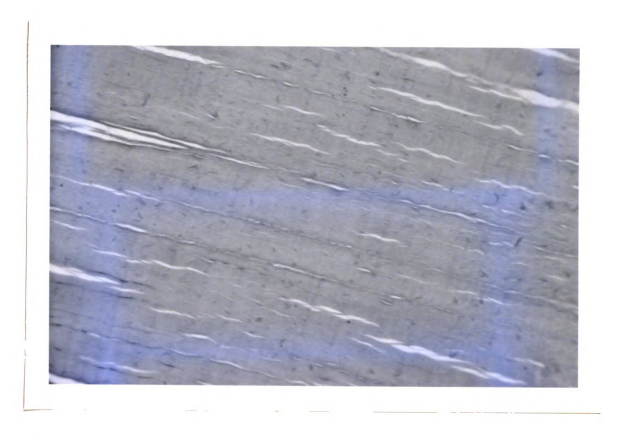
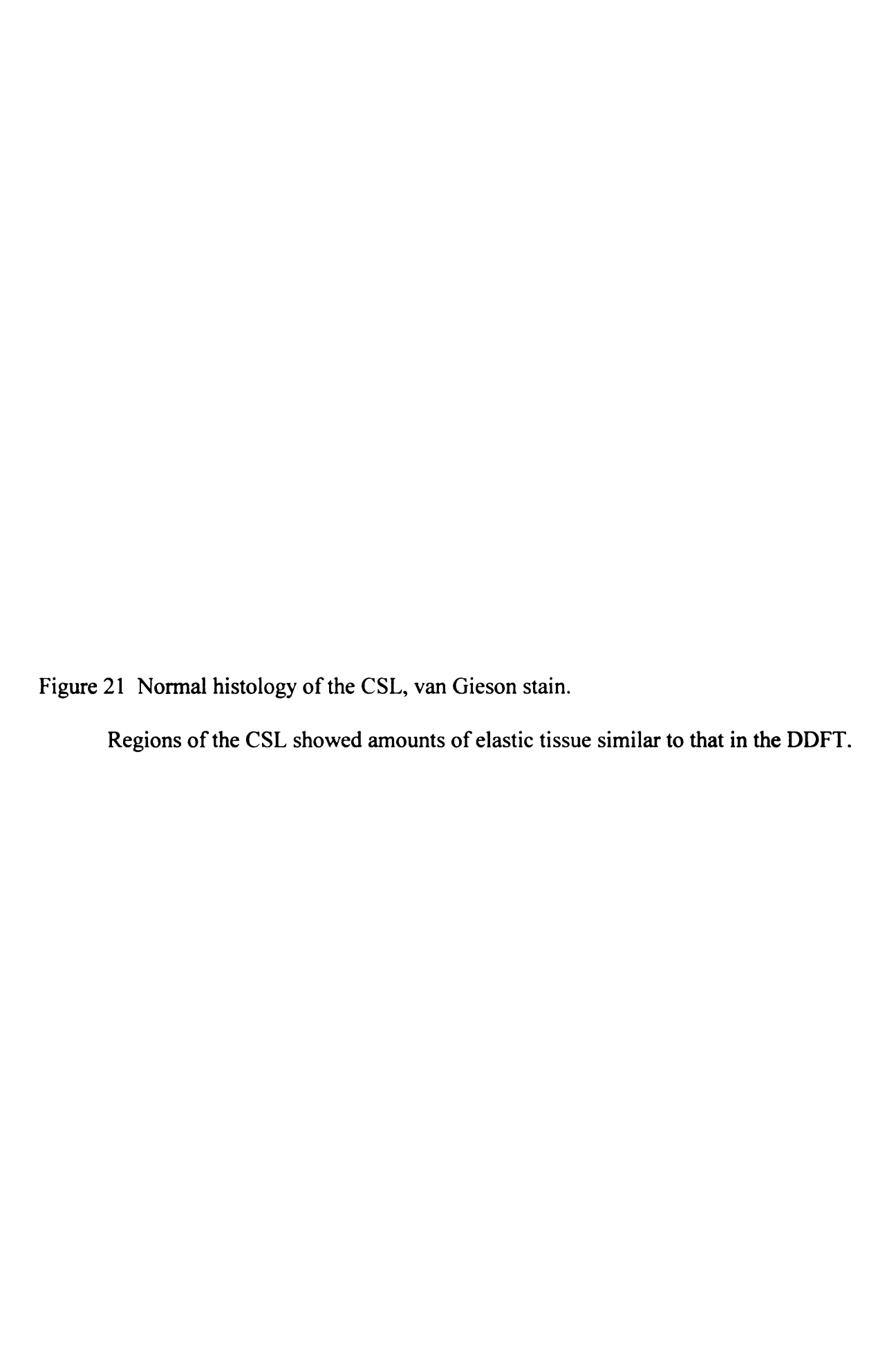


Figure 20 Normal histology of the DDFT at the flexor cortex of the navicular bone, van Gieson stain.



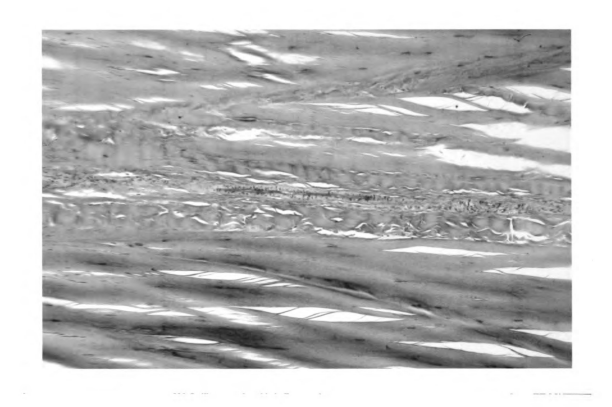


Figure 21 Normal histology of the CSL, van Gieson stain.

## SP-like immunoreactivity

Bundles of SP immunoreactive nerves were identified within the loose connective tissue septa of the DSIL/DDFT intersection with immunochemistry (Figures 22,23). When highlighted by the immunoreactively bound reaction product, single nerve fibers or bundles of nerve fibers appeared as series of black beads and were observed to course parallel to the other fibers of the DSIL. These immunoreactive nerves passed into the navicular bone proximally, as well as into the distal phalanx distally, from the DSIL/DDFT intersection. Additional collections of nerves, appearing as lattice networks encompassing vessels, innervated the vasculature coursing through the loose connective tissue septa. However, in the tissue sections of the control experiments, which were incubated either with an excess of SP or with the omission of the primary antisera, no immunoreactively labeled fibers were observed. This indicates that the primary antisera was specific to SP or a SP-like peptide as the excess SP competitively inhibited the binding of the antisera to SP present in the tissue.

After demonstrating the presence of the neuropeptide SP and the abundance of nerves in the DSIL/DDFT intersection, SP receptors in the tissue were identified using I<sup>125</sup> radioactively bound to the peptide (Bolton - Hunter SP) that then binds to its specific receptor in exposed tissues. The SP receptors were represented on radiographic film as accumulations of silver grains retained on the developed film (Figure 24a, b, c). SP receptors, as identified by silver grain accumulations, were found in the greatest concentration overlying the smaller vascular structures in the loose connective tissue of the DSIL/DDFT intersection, and the larger-sized arterioles showed significantly less binding. Dense accumulations of silver grains overlaid small vessels and their

surrounding epithelial-like cells, which together appeared to be the same structures identified as arteriovenous complexes with India ink perfused specimens (Figure 25a, b). The experimental method and resolution were not precise enough to identify if the receptors were actually located within the walls of the vessels or in the immediate surrounding tissue (epithelial-like cells. In the control tissues, which were incubated in non-radiolabeled SP in excess of I<sup>125</sup>-SP, I<sup>125</sup>-SP binding to the tissue decreased dramatically to the point of no appreciable binding (Figure 24a, b, c). The specific type of tachykinin receptor prominent in the tissue was identified using  $[sar^9, Met (O_2)^{11}]$  substance P. The tissues exposed to this peptide, a known NK1 receptor agonist, in excess of I<sup>125</sup>-SP were similar in appearance to those tissues in the control solutions, with very little binding of I<sup>125</sup>-SP, indicating a predominance of NK1 receptors for SP. The tissues taken from the dorsal hoof wall exhibited similar distribution of receptors in that the smaller resistance vessels (referring to arterioles, capillaries, and venules) displayed the most prominent receptor binding (Figure 26a, b, c). Please see the tables and graph in the appendix. Statistical analysis was not performed due to the small number (n=5, n=3, respectively) of specimens. In addition, the differences between the results from the experimental tissues and the control tissues were evident visually, without any computer aided measurements.

Figures 22, 23 DSIL with immunochemistry.

Immunochemistry using antisera to the peptide substance P identified the presence of the peptide in the tissue. The black beaded lines (arrows) coursing through the loose connective tissue septa of the DSIL and DSIL/DDFT intersection are nerves labeled for substance P.

S = loose connective tissue septa

D = dense connective tissue fibers

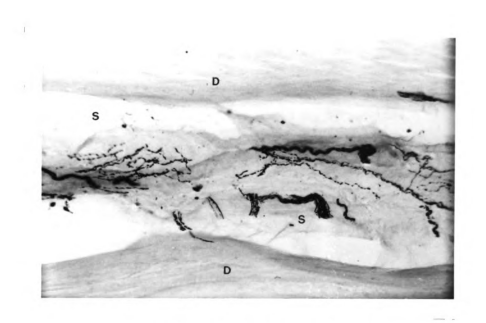


Figure 22 DSIL with immunochemistry.



Figure 23 DSIL with immunochemistry.

Figure 24a, 24b, and 24c Receptor autoradiography - SP receptor labeling.

The receptor autoradiographic technique identifies the receptors for the peptide substance P in the tissue by exposing the tissue to radiolabeled SP that binds to the receptors and causes retention of silver grains on radiographic film. The presence of the receptors is then quantitated indirectly by measuring the density of the silver grains remaining on the film. Tissue sections must be superimposed on the radiographic film to appreciate the location of the silver grains, indicating the presence of SP receptors.

**▲**= nonspecific binding

 $\Delta$  = specific binding

V = vessels

● = tissue margins

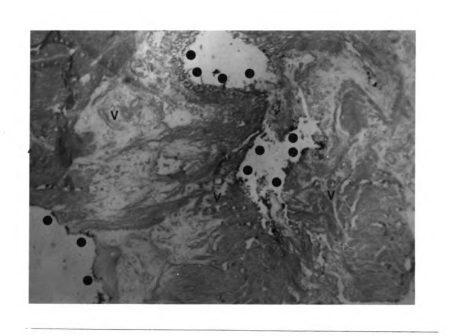


Figure 24a Receptor autoradiography - tissue.



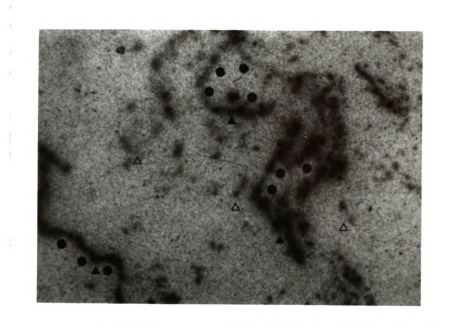


Figure 24b Receptor autoradiography - experimental/specific binding.

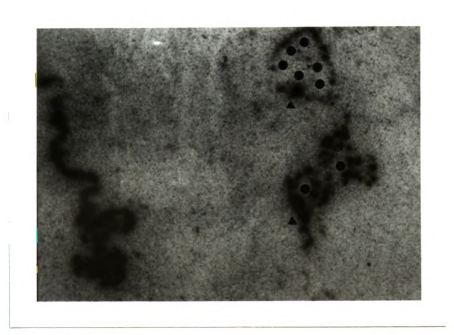


Figure 24c Receptor autoradiography - control.

Figure 25a and 25b SP receptor labeling around an AVC.

Labeling of receptors by receptor autoradiography was found to be especially dense around the AVCs. The resolution was not fine enough to determine if the receptors were actually located on the vessel walls or on the epithelial-like cells surrounding the vessels. As the vascular structures were difficult to evaluate in some sections, they were identified as AVCs by comparing the tissue to those tissues infused with India ink. (This is the same tissue section as in Figure 24).

 $\Delta$  = cross sections of AVCs

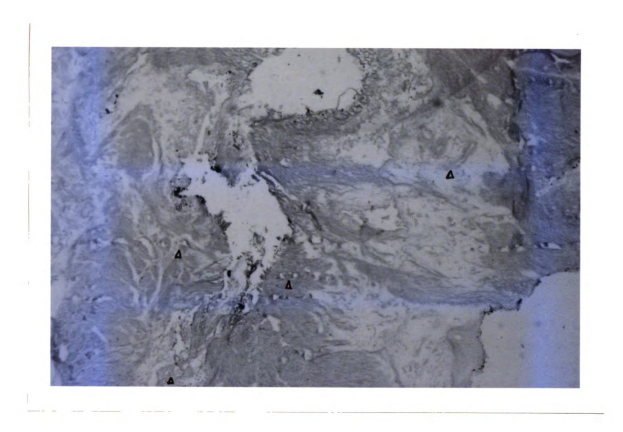


Figure 25a SP receptor labeling around an AVC - tissue.

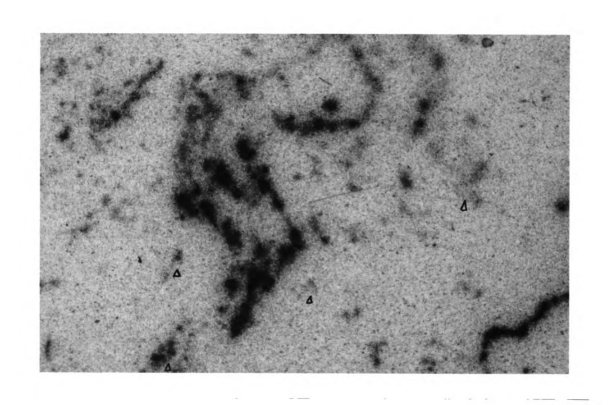


Figure 25b SP receptor labeling around an AVC - experimental/specific binding.

Figure 26a, 26b, and 26c SP receptor labeling on the dorsal hoof wall.

Some binding was present on all sections regardless of incubation solution, possibly due to binding to the epidermis. The areas of interest are the dark spots below the lamina that are located at vessels and are not present on the control film (figure 43). The binding on the lamina is considered nonspecific binding as it is the same on both experimental and control slides. The specific binding of SP on the tissues of the dorsal hoof wall, located on or around small vessels, was noted to be similar to the location of binding in the DSIL/DDFT intersection.

H = lamina of hoof wall

 $\triangle$  = nonspecific binding

= tissue margins

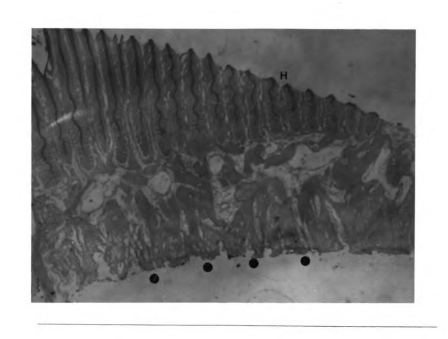


Figure 26a SP receptor labeling on the dorsal hoof wall - tissue.

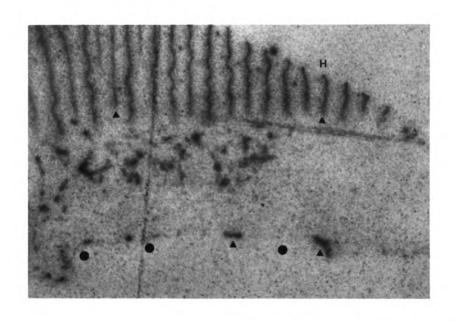


Figure 26b SP receptor labeling on the dorsal hoof wall - experimental/specific binding.

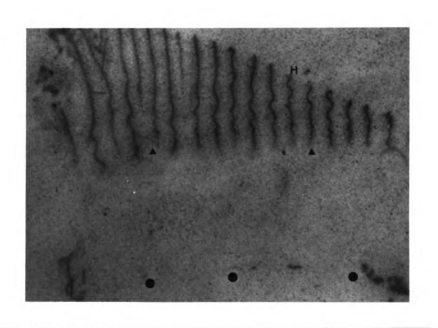


Figure 26c SP receptor labeling on the dorsal hoof wall - control.

# CGRP-like immunoreactivity

The immunochemistry experiments performed to assess the prevalence of CGRP in the tissues of the DSIL/DDFT intersection obtained results similar to those for SP. The nerve fibers and bundles of nerve fibers were identified by black lines with beading and were found within the septa of the DSIL/DDFT intersection. As with the SP, no immunoreactively labeled fibers were seen in the experiments in which the primary antisera to CGRP was omitted.

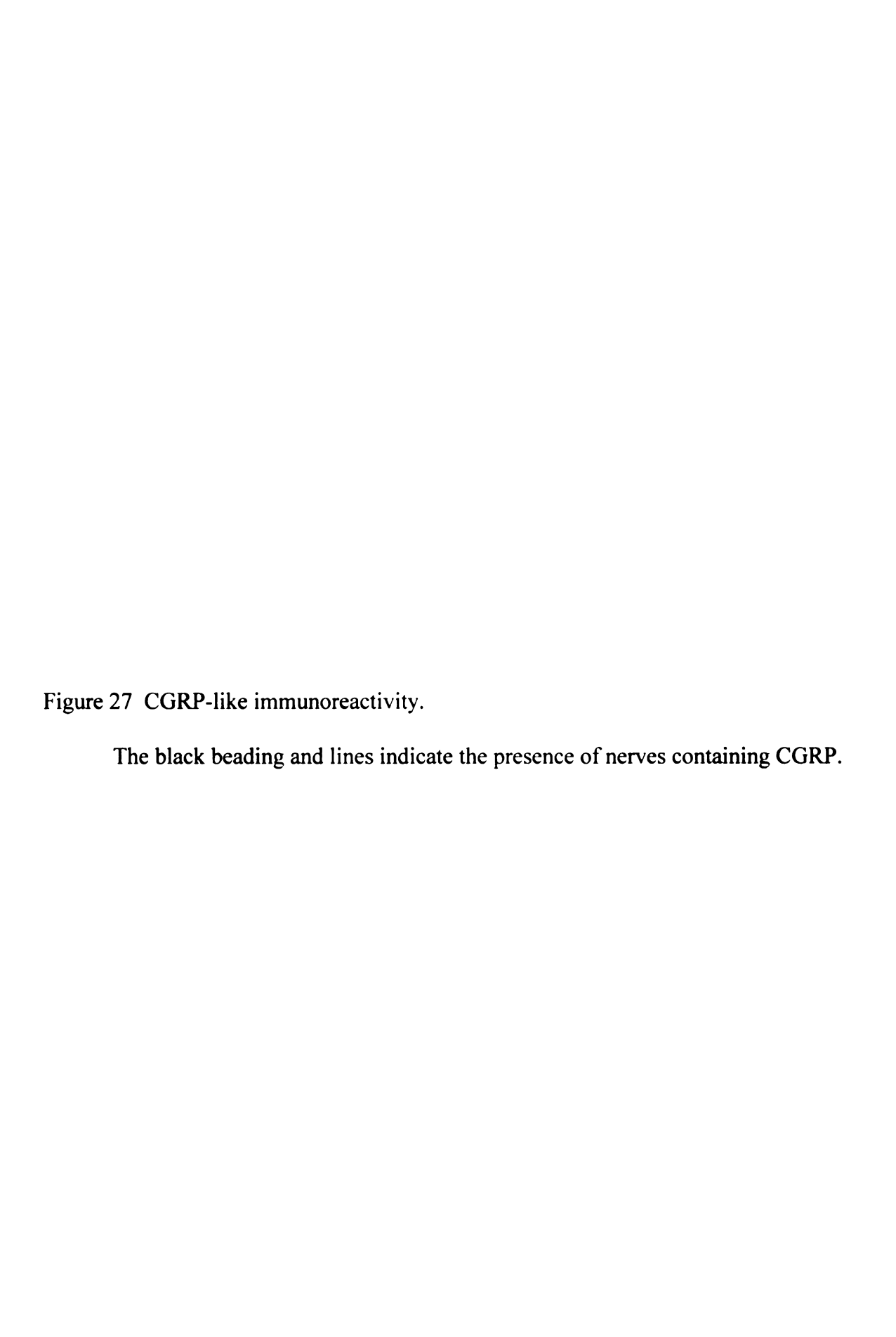




Figure 27 CGRP-like immunoreactivity.

# Non-chemically Identified Innervation

In addition to the nerves containing the specific neuropeptides SP and CGRP, other nerves present in the tissue were also identified using the gold chloride impregnation technique. This technique impregnates the axons of nerve fibers non-specifically, in contrast to SP immunochemistry that marks only a specific subpopulation of chemically-identified nerves. With the gold chloride method, the abundance of sensory and autonomic nerves present in the loose connective tissue septa of the DSIL/DDFT intersection could be visualized. The axons, which commonly existed in bundles, appeared as black lines coursing through the tissue of the DSIL/DDFT intersection (Figure 28). In other parts of the DDFT, as compared to the DSIL/DDFT intersection, fewer nerves were present between tendon fiber bundles.

Figure 28 Gold chloride impregnation.

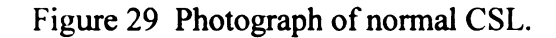
The DSIL and the DSIL/DDFT intersection were found to have a vast neural network with the gold chloride impregnation technique. The dark (almost black) fibers and bundles of fibers in the loose connective tissue of the DSIL/DDFT intersection are the nerves that have been impregnated with gold chloride.



Figure 28 Gold chloride impregnation.

# The Collateral Sesamoidean Ligament

As gross dissection of the equine foot was performed during this study, the proximal extension of the collateral sesamoidean ligament (CSL) was observed to consistently form an attachment to the second phalanx rather than to the first phalanx (Figures 29, 30). The insertion onto the second phalanx attached immediately proximal to the articulating tubercle on the palmar (plantar) surface of the second phalanx and extended in a dorsal and proximal direction along the abaxial surface of the second phalanx. At the proximal interphalangeal, or pastern, joint the CSL became a thin ribbon-like structure that fused with the joint capsule and the collateral ligaments of the pastern joint.



This photograph of the CSL in a normal horse shows its attachments to the proximal border of the navicular bone and to the abaxial portions of the second phalanx.

CSL = collateral sesamoidean ligament

3 =third phalanx

2 = second phalanx

N = navicular bone

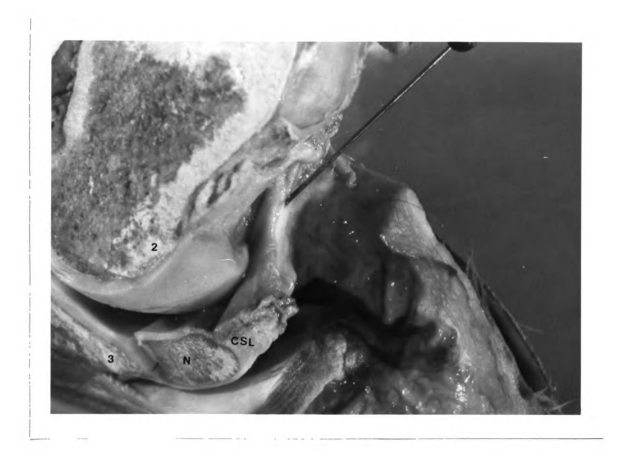


Figure 29 Photograph of normal CSL.

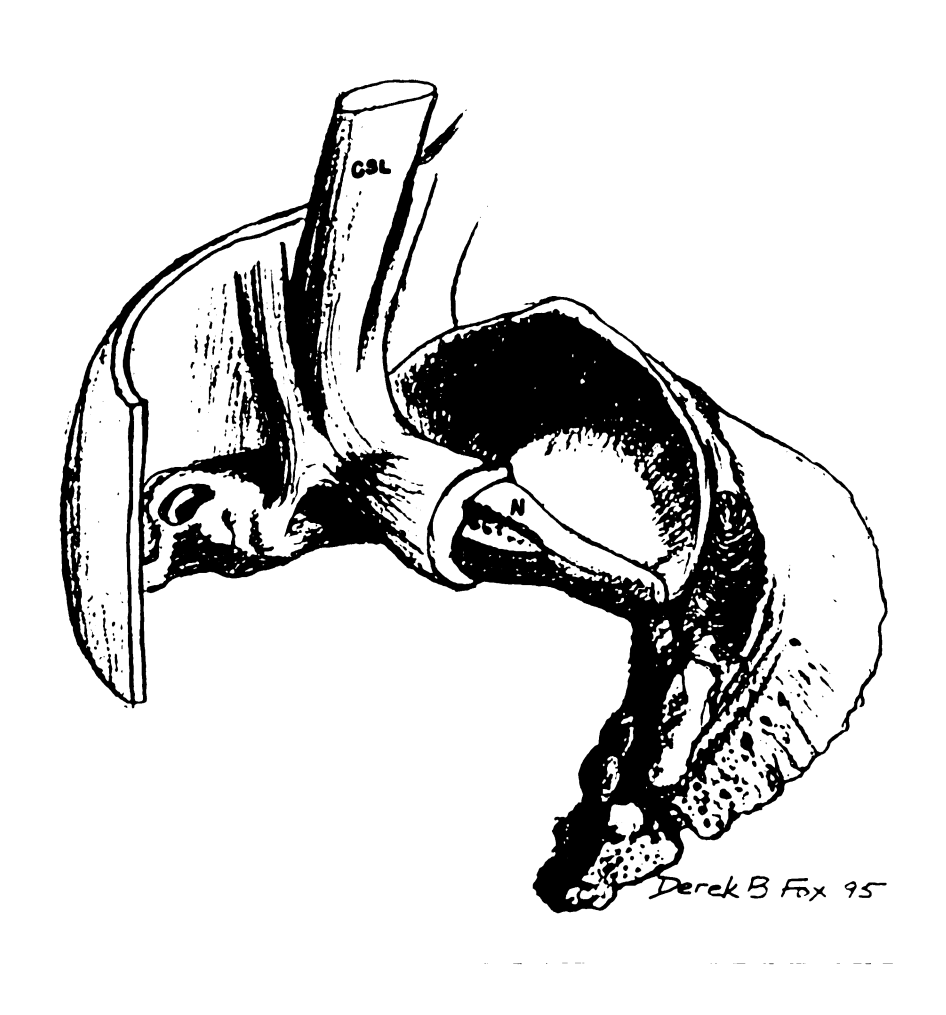


Figure 30 Illustration of normal CSL.

#### **DISCUSSION**

This study finds the DSIL/DDFT intersection to be unique in its normal macroscopic and microscopic anatomy in comparison to other tendons and ligaments The DSIL/DDFT intersection consists of dense, regular within the equine foot. connective tissue fiber bundles separated by loose connective tissue penetrating septa that contain an abundance of small blood vessels and nerves. Further evaluation of these blood vessels with the use of India ink-perfused specimens facilitated the observation of arteriovenous complexes, also within the loose connective tissue septa. The vast neural network within these septa of the DSIL/DDFT intersection, visualized with the techniques of immunochemistry and gold chloride impregnation, appears to be much more extensive than in other adjacent ligaments and tendons and to supply predominantly sensory innervation to this region. The abundant sites of action of the peptide SP, potentially released from the sensory nerve endings, are revealed with receptor autoradiography. The presence of SP receptors on blood vessels implies that SP, and perhaps other similar peptides, may have a major role in the control of blood flow through this region and other parts of the equine foot. These findings suggest a possibility for a new hypothesis on the pathogenesis of navicular syndrome.

With the discovery that the DSIL/DDFT intersection was different from other tendons or ligaments, the possibility of a normal variation from the typical was explored.

As tendons or ligaments near their insertion onto a bone, alteration in their structure is expected. The dense regular connective tissue composition should change to fibrocartilage, and then the fibrocartilage should become mineralized prior to insertion onto the bone (Dellman, 1993). However, such a description does not fit the area of the DSIL/DDFT intersection or the insertion of the DSIL/DDFT intersection onto P3.

# Histology

The DSIL/DDFT intersection was compared to the sections taken of the DDFT opposing the flexor surface of the navicular bone and at the level of the CSL, the CSL (including its insertions), and the collateral ligaments of the DIP joint. Characteristics of basic histology were evaluated, including elastin, collagen, blood vessels, and nerves. In contrast to a typical tendon or ligament composed of dense regular connective tissue, such as the DDFT, the DSIL/DDFT intersection is significantly different due to the larger fraction of loose connective tissue. This loose connective tissue in the DSIL/DDFT intersection may be due to the necessity of its presence around the many blood vessels and nerves to be discussed later.

#### Elastic Tissue

The DSIL/DDFT intersection was also shown to have relatively large amounts of elastic tissue. While elastin is known to be present in large amounts in the nuchal ligament, spinal ligaments, and large arteries, it is found only in scant amounts in most ligaments (Bloom and Fawcett, 1968). The elastin extending through the DSIL/DDFT intersection and into the dorsal portion of the DDFT distally was found to exist in greater

proportion to other fibers than the elastin in the DDFT, CSL, or collateral ligaments of the coffin joint. Such a composition allows for greater movement with rapid replacement of the distal sesamoid bone during various gaits of the horse. Furthermore, the differences in tissue composition between the DSIL and DDFT suggest the possibility that shear forces (discussed later) may exist between these two connective tissues during various stance phases from initial ground contact to dorsiflexion of the distal phalanx, creating a need for a resilient structure.

Additional examination of the histological sections of the DSIL/DDFT intersection, the more proximal DDFT, the CSL, and the collateral ligaments of the DIP joint involved the vascular and neural supplies to tendons and ligaments. Within the DSIL/DDFT intersection, the extensive networks of blood vessels and nerves were found almost exclusively in the loose connective septa uniquely present in the DSIL/DDFT intersection. As expected, these loose connective tissue septa were not found in the other ligaments and tendons, and the relative numbers of blood vessels and nerves present in these other ligaments and tendons were fewer in comparison to those observed in the DSIL/DDFT intersection. Thus, the quantity of blood vessels (including the AVCs) and nerves present in the DSIL/DDFT intersection in the loose connective tissue suggests significant functional differences between the insertional attachments of other tendons and ligaments and those of the DSIL/DDFT intersection.

## Arteriovenous Complexes

The observation of the arteriovenous complexes (AVCs) in the DSIL/DDFT intersection raises many questions as to their function. Arteriovenous anastomoses have

long been known to exist in mammals, such as in human fingers (Hale and Burch, 1960), rabbit ears (Clark and Clark, 1934), and seal skin (Molyneux and Bryden, 1978), where they are recognized as serving the role of thermoregulators, which shunt blood either from colder regions to conserve heat or to cooler regions to dissipate heat. In the horse, arteriovenous anastomoses are known to be located in the dorsal hoof wall (Molyneux, 1994), and although their function is still questioned, they may serve as thermoregulators. How they respond and to what specific substances they respond is not yet known.

The AVCs in the DSIL/DDFT intersection, unlike anastomoses in fingers, ears, or the hoof wall, most likely serve an alternative function to thermoregulation as they are located deep, or internally, within the structures of the horse foot. The DSIL/DDFT intersection is in an optimal location for control of blood flow through the foot as it spans nearly the width of the foot on the flexor surface of the distal phalanx, contacts the entire distal portion of the navicular bone, and contains the distal blood supply to that bone. More specifically, greater than three quarters of the arterial blood supply to the navicular bone pass through the DSIL and DSIL/DDFT intersection (Rijkenhuizen *et al.*, 1989a), emphasizing the importance of the blood flow through this region. Changes in the blood flow through the DSIL/DDFT intersection could be regulated by the AVCs, altering flow from or into the distal phalanx or the navicular bone in response to the abrupt pressure changes within the foot during locomotion.

#### Nerves and Neurotransmitters

Another remarkable difference between the microstructure of the DSIL/DDFT intersection and other ligaments and tendons is the abundance of nerves, located within

the loose connective tissue septa, in the DSIL/DDFT intersection. Similar in significance to the vascular structures in this region, which may impact the control of blood flow, these nerves likely transmit crucial sensory input during phases of locomotion and standing, including pain sensation with lameness affecting this region. In addition, these nerves (shown to be present with gold chloride impregnation and immunochemistry) supply the neuropeptides to the specific receptors, such as for SP (shown to be present with receptor autoradiography).

After further consideration of these nerves and neurotransmitters, substance P can be hypothesized to act on the blood vessels of the DSIL/DDFT intersection due to the combined results of immunochemistry and receptor autoradiography. One necessary component is that SP be present within the nerves of the DSIL/DDFT intersection, which was demonstrated by previous experiments in our laboratory (Bowker, 1995b) and reconfirmed in the present study with immunochemistry. However, the presence of the peptide SP in nerves does not indicate that the peptide binds and acts in the same tissue as these fibers are known to convey sensory information to the spinal cord. Thus, the technique of receptor autoradiography was necessary to reveal the presence of specific receptors for this peptide within the tissues of the equine foot. As stated in the methods, three solutions were used, into which adjacent sections of tissue were placed. The first solution, containing radiolabeled SP, resulted in identification of SP receptor locations in the tissue as SP binds to all three types of neurokinin receptors (NK1, NK2, and NK3), although not with the same affinity (Mantyh, 1989). The second solution, however, of radiolabeled SP and non-radiolabeled SP (in excess), served as a control solution, in which those tissues incubated showed no specific binding of radiolabeled SP, indicating

competitive inhibition by the non-radiolabeled SP. The third and final solution, which incubated the tissues with radiolabeled SP and the NK1 (neurokinin 1) agonist or antagonist in excess, served to identify the receptor types in the tissue, again acting on the premise of competitive inhibition. Previous studies in our laboratory revealed that the predominant receptor type for SP in the horse (almost to the exclusion of two other tachykinin receptor types that can be identified with receptor autoradiography) was NK1 (Sonea et al., 1993). The previous studies revealed no appreciable difference between those tissues incubated in radioactively labeled SP alone and radioactively labeled SP plus an NK2 agonist. This finding does not, however, indicate that NK2 receptors were not present in the tissue or if the NK2 agonist (SP) simply did not bind to NK2 receptors with any significant affinity. The tissue incubated in the solution with the NK1 agonist showed very little to no specific binding of radiolabeled SP to receptors, and thus the results were similar to those for tissues incubated in the control solution (please see figure 24). As a result, our conclusion is that SP exposed to the DSIL/DDFT intersection bound to the NK1 receptors present almost to the exclusion of NK2 or NK3 receptors, or that few, if any, NK2 nor NK3 receptors were present.

In addition, the presence of substance P receptors on the AVCs and/or their surrounding epithelial-like cells draws attention to the AVCs' possible roles in alteration or regulation of blood flow as a response to noxious stimuli. These AVCs may be dilated in response to SP, depending on their nature (arteriole or venule), and the effect of many AVCs on the blood flow to or from the navicular bone or other nearby areas would be dramatic (see discussion of SP below). The importance of these AVCs, potentially as pressure regulatory devices in the DSIL/DDFT intersection, may relate to navicular

syndrome in which higher intramedullary pressures within the navicular bone are observed in comparison to normal horses (Kobluk *et al.*, 1995). In preliminary observations of histology and receptor autoradiography performed on three horses diagnosed with navicular syndrome, there appears to be a reduction in the number of AVCs and SP receptors in the DSIL/DDFT intersection of these horses (unpublished observations). This finding may reflect a destruction of these structures during the disease process and would be consistent with our hypothesis. Fewer SP receptors would be available to respond to stimuli to protect the tissue from damage, thereby propagating the pathological process initiated within the DSIL/DDFT intersection.

The presence of SP receptors on the small resistance vessels (arterioles, capillaries, and venules) in the dermis of the dorsal hoof wall leads to the impression that SP receptors may be common to many of these small vessels in the horse foot. In the dorsal hoof wall, SP is likely to play a role in inflammatory disease states (e.g. laminitis) as in the DSIL/DDFT intersection. (Please see tables and graph in the appendix). As a result of the analysis of the receptor distribution on the vessels of these two very different areas of the horse foot, the DSIL/DDFT intersection and the dorsal hoof wall, it may be suspected that SP receptors have a predilection for these resistance vessels in the foot.

The majority of the nerves innervating the horse foot via the palmar nerves have been shown to be unmyelinated nerves, present in a ratio of almost 5 unmyelinated nerves to each myelinated nerve (Bowker et al., 1995), which is consistent with findings in other species (McLachlan and Janig, 1983). Approximately 25% of these unmyelinated nerves provide sympathetic innervation to the foot, which supplies motor function to the blood vessels of the foot to cause vasoconstriction (McLachlan and Janig, 1983). The

remaining 75% (approximately) of the nerves provide sensory function to the foot, which represents a large number of nerves considering the lack of muscle in the distal limb. These nerves are likely to serve a dual function of relaying information from the periphery to the spinal cord, i.e., classic sensory function, and local impulses back to the periphery, i.e., classic motor function.

Primary afferent nerves are traditionally thought to transmit impulses in an orthograde direction. However, afferent nerves have been shown to have an efferent effect by transmitting in an antegrade direction, causing a release of neuropeptide from the peripheral processes of sensory nerves (Weihe, 1990; Taylor and Dierau, 1991). The afferent neuron and its peripheral processes are not a simple unit to relay sensory information from the periphery to the spinal cord, but act to convey information to both the periphery (an efferent function) and centrally to the spinal cord (an afferent function). The efferent function of the sensory nerves would serve to stimulate the receptors in the periphery, such as the SP receptors identified with receptor autoradiography.

Sensory and autonomic nerves located in the tissues of the DSIL/DDFT intersection, as shown with the gold chloride impregnation technique, are necessary for the first step toward the release of substance P. Once a stimulus is received by one of the sensory nerves, it is propagated in a prodromal direction; however, other sensory branches of the nerve receive antidromic stimulation as the initial impulse is propagated (Figure 31). This stimulation of the sensory nerve fibers creates a release of SP that can then bind to the NK1 receptors present in the tissue, mediating the release of endothelium-derived releasing factor (EDRF) from endothelium and histamine in addition to mediating other events that occur with neurogenic inflammation (Edvinsson,

1993). This axon reflex provides a means for a rapid response (vasodilation) to a noxious stimulus without CNS acknowledgment, which would decrease the efficiency of the response.

Such nociceptor feedback loops described in the previous paragraph could be present locally in the tissue to cause release of peptides (SP, CGRP), resulting in vasodilation (SP can cause vasoconstriction in certain vascular beds). The vasodilation occurring with SP is hypothesized to be mediated by nitric oxide (Busse and Mulsch, 1991). SP or a metabolic by-product may also be involved in the alterations in the capillary bed and post capillary venules during plasma extravasation. The binding of SP and other transmitters, not all of which have been identified, would alter the volume and rate of blood flow through the DSIL/DDFT intersection, affecting the flow through a large area in the foot.

The importance of such a reflex in the horse foot may be realized when considering that the time between each foot's consecutive impacts is only a fraction of a second. Any responses necessary to adjust the conditions within the foot would be much more effective and beneficial with more immediate results.

Figure 31 Axon Reflex.

Peripheral sensory neurons may serve to both relay information to the central

nervous system and transmit signals back to the periphery to cause release of various

neuropeptides. This type of axon reflex would result in rapid response of the tissue at the

site of stimulation. The peptide substance P, if released from the peripheral nerves onto

the NK1 receptors on or near the blood vessels, would override the stimulus of the

sympathetic nervous system to vasoconstrict, causing vasodilation and promoting

neurogenic inflammation.

The drawing on the right represents a lateral view of the brain and spinal cord.

The drawing on the top left represents a parasagittal view of the horse foot showing the

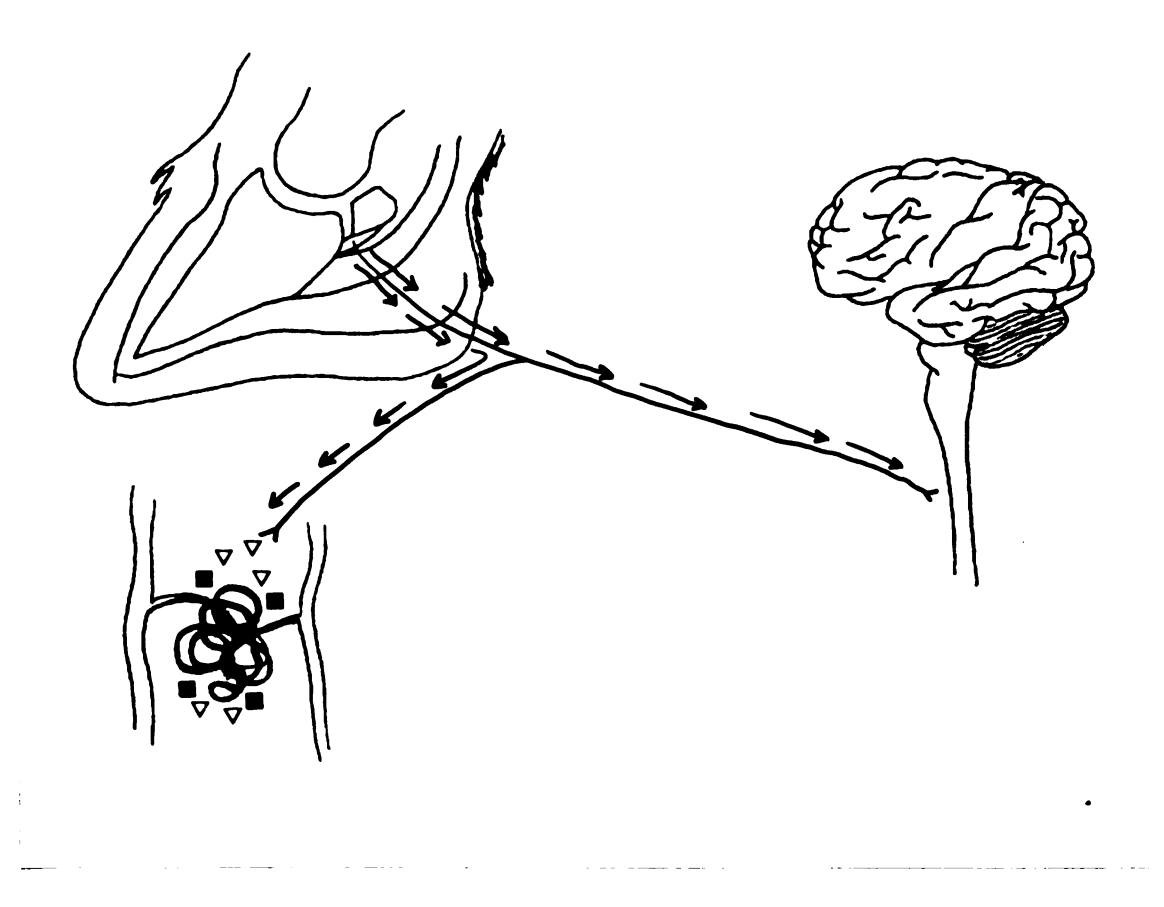
distal end of P2, P3, navicular bone, DSIL, DSIL/DDFT intersection, and DDFT. The

drawing on the bottom left represents an AVC with a supplying vessel, capillary glomus,

and collecting vessel.

 $\blacksquare$  = NK1 receptor

 $\nabla = SP$ 



į

Figure 31 Axon Reflex.

## Function of the DSIL/DDFT Intersection

Considering the described structure of the DSIL/DDFT intersection with its unique loose connective tissue septa containing many blood vessels and nerves, and in particular the AVCs and the abundance of sensory nerves, the function of the DSIL/DDFT intersection must be carefully contemplated. The position of the DSIL/DDFT intersection in the foot, spanning the width of the third phalanx and harboring vascular and neural supply to the navicular bone, is optimal for regulation of blood flow, which could be both sensed and controlled with the vast neural network present. Blood flow courses through the abaxial sides of the DSIL/DDFT intersection while venous drainage from the sole also passes through the DSIL/DDFT intersection to the ungual cartilage (Bowker et al., 1998b). Normally the majority (i.e. 75% (Rijkenhuizen et al., 1989a)) of the blood flow to and from the navicular bone courses through the tissues that we have termed the DSIL/DDFT intersection. Movement of blood and pressure shifts within this region must be frequent and high during various locomotory gaits in the horse. To accommodate such activity, the microanatomy of this region must be structured to rapidly dissipate the transient high pressure to prevent vessel rupture as well as maintain sufficient blood flow to the tissues to provide nourishment and waste removal. In addition to other pressure affectors, the AVCs and their associated SP innervation appear to be in position to aid in the prevention of transient peak vascular pressures to and from the navicular bone in accordance with pressure changes occurring during weight bearing and non-weight bearing phases of the stride. The peptide SP in the horse foot produces a vasodilation (Pelletier and Bowker, unpublished data). In navicular syndrome, damage to the DSIL/DDFT intersection with disruption of the AVCs and SP

receptors (Bowker and Van Wulfen, unpublished observations) may be related to the high intramedullary pressures in the navicular bone (Kobluk *et al.*, 1995), although which event was first to occur can only be surmised.

### Forces on the DSIL/DDFT Intersection

Further review of the DSIL/DDFT intersection involves the forces and stresses placed on the DSIL/DDFT intersection itself. As previously mentioned, the DSIL and DSIL/DDFT intersection are subjected to extreme stress when the navicular bone bears much of the weight of the horse (Bowker et al., 1998). During dorsiflexion of the distal phalanx, the middle phalanx rotates within the DIP joint, pushing the navicular bone into position as a portion of the weight-bearing surface of the joint (please see figure 4). Additional evidence from our laboratory has shown that the load on the navicular bone increases significantly during dorsiflexion (Bowker et al., 1998). The forces on the navicular bone are then transferred to the suspensory ligaments, the CSL and DSIL. The DSIL yields slightly to absorb force (Dyce, 1987), which allows the navicular bone to be pushed slightly palmarly (or plantarly) and/or distally. This displacement of the navicular bone changes the direction of force on the insertion of the DSIL/DDFT intersection. Although the navicular bone has been previously proposed to create a constant angle of insertion of the DDFT onto the distal phalanx (Rooney, 1969), this angle may change when the limb is in dorsiflexion and the navicular bone serves its crucial function as a major weight-bearing surface (unpublished observations). The DSIL and DSIL/DDFT intersection (and CSL proximally) must maintain this weight-bearing surface by withstanding the change in angle of insertion and extreme weight placed on the navicular

bone; for example, when landing after a jump. These dynamic functions of the navicular bone and its suspensory ligaments suggest that the elastic tissue present in the DSIL/DDFT intersection is more effective than purely collagen as the DSIL/DDFT intersection must quickly respond between strides in a horse's gait.

During dorsiflexion in the terminal phase of the stride, shear forces between the DSIL and DDFT may develop at the DSIL/DDFT intersection due in part to the differences in tissue composition between these two connective tissue structures. Shear forces may also occur if unequal pull is placed on the DDFT compared to the DSIL. Such shear forces that develop would potentially be significant enough to disrupt the integrity of the tissues, including vessels and nerves, on a microscopic level.

Other forces, to which the DSIL/DDFT intersection is exposed, are basic compression and concussion as the horse stands and/or lands on the foot. These forces would be equal to the horse's weight plus the momentum of the foot and body on impact.

Any faults in conformation of a horse's feet could affect the intensity of the forces on the structures of the feet, contributing to pathology.

During these dynamic changes in forces (shear, compression, concussion) in the foot, the structures in the DSIL/DDFT intersection would be exposed to the extreme stress of deformation and reformation. Such stress could cause microstructural damage to fragile structures such as loose connective tissue, blood vessels, and nerves. Damage to these structures would compromise the neurovascular supply to the surrounding structures, including the navicular bone. This, in turn, may affect the means of pressure dissipation in this region. Stimuli and/or damage to the sensory nerves of the DSIL/DDFT intersection would cause the release of SP due to the axon reflex previously

described and result in inflammation in the tissue. These inflammatory changes in the DSIL/DDFT intersection would also affect the navicular bone, as the blood supply to and from the navicular bone (and the AVCs) would be compromised. Such a hypothetical course of events would result in the initiation of the pathogenesis of navicular syndrome (Figure 32).

The forces placed on the individual limbs may also explain the predominance of navicular syndrome in front limbs versus hind limbs. The front limbs support 60% of an animal's weight, which obviously would strain the ligaments and tendons of the front limbs more severely. In addition, compared to the pelvic limb, fewer distal arteries supplying the navicular bone are present within the DSIL of the thoracic limb (James *et al.*, 1980). As changes within the DSIL/DDFT intersection may compromise the blood supply to the navicular bone, the foot with fewer vessels may show clinical signs more rapidly. Both the greater forces and fewer arteries may relate to the higher incidence of navicular syndrome in the thoracic limbs.

Additional factors must influence the occurrence of navicular syndrome as not all horses develop problems related to navicular syndrome. The predisposing elements may include breed, foot conformation, hoof trimming and shoeing, working surfaces, level of work, and more. The horses at highest risk may be difficult to identify due to many compounding factors.

Figure 32 Hypothesis flow chart.

This simplified flow chart follows the basic outline of this hypothesis to help explain the origin of the pain in navicular syndrome that causes lameness.

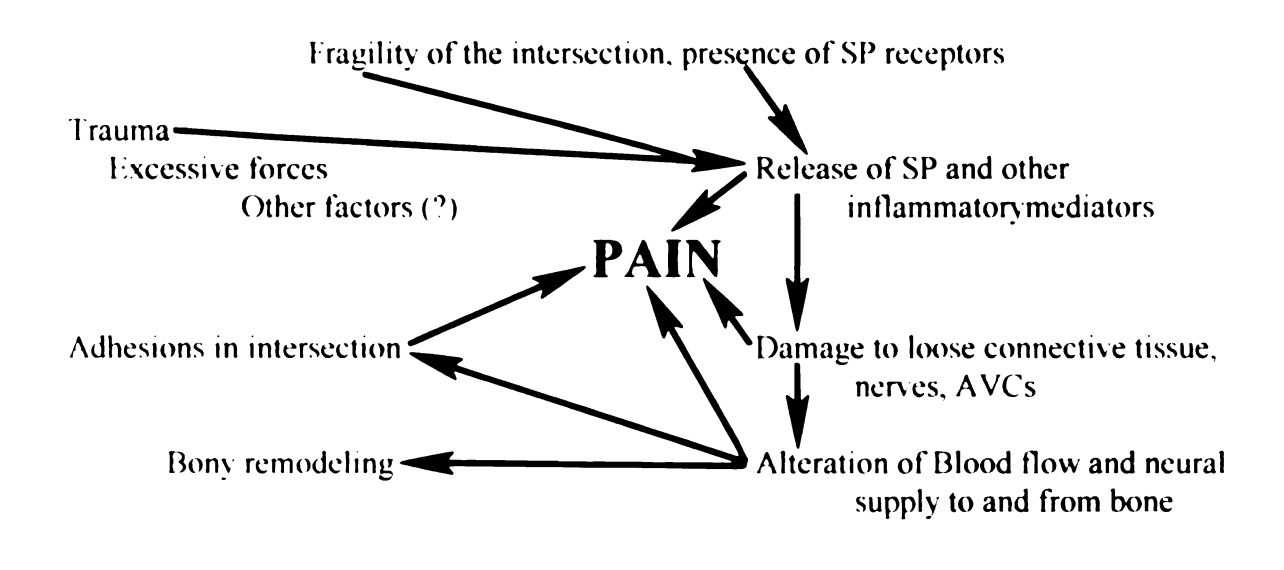


Figure 32 Hypothesis flow chart.

## Previous Hypotheses

Following a consideration of the current findings, the hypotheses that have been presented in the past for the pathogenesis of navicular syndrome should be reviewed, considering their ability to explain the pathology found with navicular syndrome.

The hypotheses (Ostblom et al., 1989a; Pool et al., 1989) that concentrate on the pressure of the DDFT against the navicular bone first of all have a critical shortcoming. They do not consider the DSIL, despite its unique anatomy, as a major determining factor in the healthy or diseased state of the navicular bone. The DSIL and its intersection with the DDFT have not previously been examined closely, despite their intimate relation to both the distal DDFT and the navicular bone. In addition, although the DDFT might logically subject the flexor cortex of the navicular bone to high pressures during locomotion, no significant pressure change on the navicular bone from the DDFT has been recorded between gaits in the horse (Schryver, 1978). This observation is consistent with more recent observations that the contraction of the DDFT muscle only occurs during the first half of the stride and not near the terminal portion of the stride (Konsgaard, 1982). However, with the present observation of the CSL's attachment to the middle phalanx, a greater compression between the navicular bone and the distal phalanx may occur than would be expected with an attachment to the proximal phalanx. This compression may affect the DSIL/DDFT intersection and result in changes within P3 (Bowker et al., 1998a).

The lesions found in and around the navicular bursa of horses with navicular syndrome appear to be consistent with the pathology seen in degenerative joint disease (DJD). Descriptions of DJD focus on the changes occurring in the articular cartilage,

subchondral bone, and synovial lining of the joint capsule (Carlton, 1995). However, DJD does not seem to account for any changes occurring in the DSIL (Stashak, 1987; Kobluk *et al.*, 1995). In addition, although DJD can occur to some degree with no apparent cause in aging animals, an event usually instigates DJD within a joint. As ligamentous injury resulting in instability in the joint is a common factor that can result in DJD, it is possible that damage sustained by the DSIL and DSIL/DDFT intersection (as previously described) would result in enough instability to cause DJD.

In examination of the DSIL, Colles and Hickman (1977) found what appeared to be thrombi in the vessels that supplied the navicular bone and concluded that such compromise to the vasculature could cause ischemia to the navicular bone. Despite the acknowledgment that the DSIL may have a role in the pathogenesis, a lack of repeatability has discounted this hypothesis (Pool *et al.*, 1989; Ostblom, 1989; Ostblom *et al.*, 1989; Hickman, 1989; MacGregor, 1989). Also, some pathological findings have not been consistent with ischemia (Rooney, 1969; Pool *et al.*, 1989). However, the structures referred to as thrombi by Colles may have been the normal vascular structures (such as AVCs) that were destroyed due to inflammation, a suspected component of navicular syndrome.

Despite the promising conclusions of the studies examining occlusion of the distal vasculature by Rijkenhuizen (1989e), these reports did not explain the cause of the problem, nor were the experimental horses clinically lame. The cause of the compromise of the vasculature is still elusive.

### Local Anesthetic

Both the structure of the DSIL/DDFT intersection and the possible pathology that may occur in the DSIL/DDFT intersection during navicular syndrome help provide an explanation for the results seen after a local anesthetic injection into the distal interphalangeal (coffin) joint (Dyson and Kidd, 1993). Dense regular connective tissue, such as that of which ligaments are composed, would prevent the diffusion of anesthetic. but loose connective tissue allows local anesthetic to diffuse through it. Thus, the septa in the DSIL/DDFT intersection, which are continuous and connected stretching from the DIP joint to the navicular bursa, allow the local anesthetic to penetrate through the DSIL and DSIL/DDFT intersection and eventually enter the navicular bursa. This observation that local anesthetic can diffuse from the DIP joint suggests that the local anesthetic injected for diagnostic purposes may diffuse beyond the confines of the synovial cavity to desensitize structures in the foot other than exposed joint surfaces (Bowker, Linder, Van Wulfen et al., 1996). However, no direct communication between the DIP joint and the navicular bursa exists (Calislar and St. Clair, 1969; Gibson et al., 1990). The diffusion path of the local anesthetic solution appears to be through the DSIL to the DSIL/DDFT intersection and then along the dorsal surface of the DDFT, rather than directly into the navicular bursa from the ventral surface of the DSIL (Bowker, Linder, Van Wulfen et al., 1996). An important note, however, is that the nerves supplying the sensory function to the DSIL/DDFT intersection, DSIL, and navicular bone are located within the septa through which the anesthetic is passing. Thus, any painful stimulus from a diseased DSIL or navicular bone will be reduced or eliminated before the local anesthetic even reaches the navicular bursa. Such a diffusion of local anesthetic solution from the DIP joint through the connective tissues of the DSIL/DDFT intersection may account for the different effects of the local anesthesia reported at 5 minutes and at later times of 15-20 minutes (Dyson and Kidd, 1993). The effects observed at 5 minutes post injection are likely due to the more direct effects of the local anesthetic on the DIP joint synovium, any exposed surfaces, and the immediate underlying connective tissues of the joint cavity. The effects observed much later would be due to the diffusion of the local anesthetic into deeper tissues, including portions of highly innervated ligaments (DSIL and DSIL/DDFT intersection), thus causing desensitization of portions of the distal sesamoid bone, the distal phalanx, and other more distal structures in the foot.

### **CONCLUSION**

The DSIL and DSIL/DDFT intersection were not found to have the expected histological composition of a typical ligament, but instead were composed of many loose connective tissue septa separating dense connective tissue fibers. In addition, the loose connective tissue contained extensive networks of blood vessels and nerves that, due to the relatively small amount of dense connective tissue, may be susceptible to damage from stress placed on the DSIL/DDFT intersection. The sensory nerves present were further identified as containing the neuropeptide SP, and specific (NK1) SP receptors were identified in the tissues surrounding novel AVCs. Such an anatomical arrangement provides the means for an inflammatory response to noxious stimuli that could result in changes in the vascular supply to the surrounding area.

Navicular syndrome is a very complex pathological disorder with an undefined etiology. Former hypotheses that have been proposed fail to allow for the many components and variations in the syndrome. However, as a result of the morphological observations described in the present thesis, most of the clinical, radiographic, and pathologic findings previously reported in navicular syndrome can be explained by the ideas presented in this thesis concerning the DSIL/DDFT intersection. While a study into the initial changes seen with navicular syndrome would be informative and challenging, it would be difficult, as well as cost prohibitive, as euthanasia is not generally a

consideration at the time of initial diagnosis. Until more precise and accurate imaging modalities are developed that can more specifically locate the site of initial changes, the exact cause and effect relationships will be difficult to determine.

# **APPENDIX**

### **APPENDIX**

The following tables list the values that were calculated from the raw measurements obtained with microdensitometry. The first table consists of values from the DSIL/DDFT intersection of three horses. The second table is taken from the values from the dorsal hoof wall of five horses. The third table averages the values from the first two tables, which were combined due to the similarity in location of the receptors. The graph uses the values from the third table.

The nonspecific binding values were expected to be high as no receptors were necessary for the binding to occur. In addition, the nonspecific binding values were similarly high for all tissue sections, as was expected because competitive inhibition does not affect nonspecific binding as it affects binding to receptors.

The values in the following tables are listed in nCi (nano Curie), which is a measurement of radioactivity. These numbers correspond in direct proportion to the amount of binding of SP\*.

SP\* = SP bound to radioactive iodine. The numbers in this column represent the tissue samples that were incubated in the solution with SP\*.

SP\* + SP = radioactive SP in addition to a 10 fold excess of unmarked SP.

SP\* + NK1 = radioactive SP in addition to a 10 fold excess of the NK1 receptor agonist.

Table 1 Receptor autoradiography data of DSIL/DDFT intersection.

Horse 1	SP*	SP* + SP	SP* + NK1
Background	-0.2382	-0.2941	-0.2486
Nonspecific	8.7338	8.8103	9.3767
Tissue	0.1136	0.2799	0.7859
Vessels	2.2142	0.2066	0.2704
Horse 2	SP*	SP* + SP	SP* + NK1
Background	0.0873	-0.0827	-0.2556
Nonspecific	8.7142	8.5047	6.3693
Tissue	0.2252	0.1358	0.3806
Vessels	3.8688	0.2990	0.4110
Horse 3	SP*	SP* + SP	SP* + NK1
Background	0.0769	-0.2346	-0.0681
Nonspecific	2.5389	1.8390	0.8400
Tissue	0.1755	-0.1302	0.0650
Vessels	4.6564	0.1705	0.2322

Table 2 Receptor autoradiography data of hoof wall.

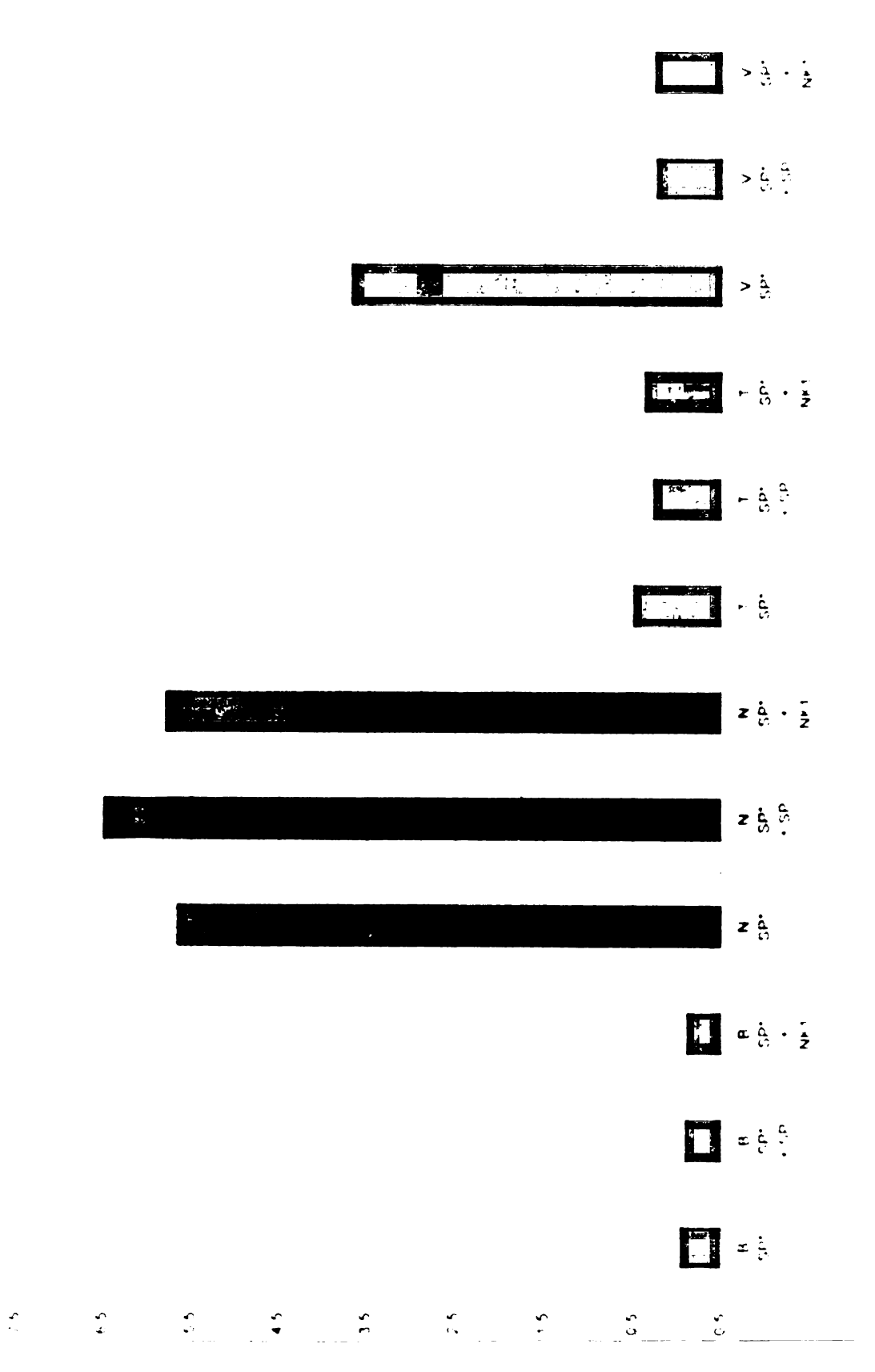
			** · · · · · · · · · · · · · · · · · ·
Horse 4	SP*	SP* + SP	SP* + NK1
Background	0.1508	0.0266	0.0043
Nonspecific	4.4853	7.4039	7.5135
Tissue	0.6831	0.4123	0.4630
Vessels	4.4960	0.2382	0.3489
Horse 5	SP*	SP* + SP	SP* + NK1
Background	0.0695	0.0443	-0.1288
Nonspecific	5.2849	5.5060	5.5675
Tissue	0.6822	0.7751	0.6961
Vessels	1.6448	0.2675	0.2323
Horse 6	SP*	SP* + SP	SP* + NK1
Background	-0.2222	-0.0966	-0.2021
Nonspecific	4.6725	6.6068	4.0881
Tissue	0.9796	0.2100	0.1528
Vessels	5.7272	0.1543	0.1028
Horse 7	SP*	SP* + SP	SP* + NK1
Background	-0.3485	-0.1867	-0.2045
Nonspecific	5.2317	6.8557	6.8832
Tissue	0.8109	0.5081	0.2649
Vessels	2.8932	0.0094	0.1193
Horse 8	SP*	SP* + SP	SP* + NK1
Background	0.1971	0.1531	0.3130
Nonspecific		•	
Tissue	0.4219	0.1419	0.2731
Vessels	4.0522	0.7126	0.5140



Table 3 Averages of tables 1 and 2.

Averages	SP*	SP* + SP	SP* + NK1
Background	-0.0284	-0.0838	-0.0988
Nonspecific	5.6659	6.5038	5.8055
Tissue	0.5115	0.2916	0.3852
Vessels	3.6941	0.2573	0.2789

## Graph of Table 3.



**BIBLIOGRAPHY** 

### **BIBLIOGRAPHY**

Adams, O.R. (1974) Lameness in Horses. Lea & Febiger: Philadelphia. 260-275.

Bloom, W., Fawcett, D.W. (1968) <u>A Textbook of Histology</u>. W.B. Saunders Company: Philadelphia, PA. 162-163, 189-190.

Bowker, R.M., Van Wulfen, K.K., and Grentz, D.J. (1995a) "Nonselectivity of local anesthetics injected into the distal interphalangeal joint and the navicular bursa." *AAEP Proceedings*, 41, 240-242.

Bowker, R.M., Linder, K., Sonea, I.M., and Holland, R.E. (1995b) "Sensory innervation of the navicular bone and bursa in the foal." *Equine vet. J.* 27 (1), 60-65.

Bowker, R.M. and Van Wulfen, K.K. (1996) "Microanatomy of the intersection of the distal sesamoidean impar ligament and the deep digital flexor tendon: A preliminary report." *Pierdeheilkunde*, 12 (4), 623-627.

Bowker, R.M., Linder, K., Van Wulfen, K.K., and Sonea, I.M. (1997) "Anatomy of the distal interphalangeal joint of the mature horse: relationships with navicular suspensory ligaments, sensory nerves and neurovascular bundle." *Equine vet. J.* 29 (2), 126-135.

Bowker, R.M., Atkinson, P.J., Atkinson, T.S., and Haut, R.C. (1998a) "Evidence of High Contact Pressures and Tissue Stresses in Navicular and Coffin Bones During Digital Dorsiflexion: The potential relation to navicular syndrome". Submitted to AAEP 1998.

Bowker, R.M., Van Wulfen, K.K., Springer, S.E. (1998b) "Functional anatomy of the cartilage of the distal phalanx and digital cushion in the equine foot and a hemodynamic flow hypothesis of energy dissipation". AJVR, Vol 59, 961-968.

Brinker, W. O., Permeatti, D. L., and Flo, G.L. (1983) <u>Handbook of Small Animal Orthopedics and Fracture Management</u>. W.B. Saunders Company: Philadelphia, PA. 286-288.

Busse, R. and Mulsch, A. (1991) "Endothelium-derived relaxing factor: Nitric oxide". Molecular Aspects of Inflammation. H. Sies. Springer-Verlag, Berlin. 189-205.

Calislar, T. and St. Clair, L.E. (1969) "Observations on the navicular bursa and the distal interphalangeal joint cavity of the horse." J. Am. vet. med. Ass. 154, 410-412.

Carlton, W.W. and McGavin, M.D. (1995) <u>Thomson's Special Veterinary Pathology, Second Edition</u>. Mosby - Year Book, Inc.: St. Louis, MO. 430.

Caron, J.P., Bowker, R.M., Abhold, R.H., Toppin, D.S., Sonea, I.M., and Vex, K.B. (1992) "Synovial innervation of the equine middle carpal joint." *Equine vet. J.* 24, 364-366.

Clark, E.R. and Clark, E.L. (1934) "Observations on Living Arterio-Venous Anastomoses as seen in Transparent Chambers Introduced into the Rabbit's Ear". The American Journal of Anatomy. Vol 54, No 2. 229-286.

Colles, C.M. and Hickman, J. (1977) "The arterial supply of the navicular bone and its variations in navicular disease." *Equine Vet. J.* 9, 150-154.

Colles, C.M. (1979) "Ischaemic necrosis of the navicular bone and its treatment." Vet. Rec. 104, 133-137.

Dellman, H.D. (1993) <u>Textbook of Veterinary Histology, Fourth Edition</u>. Lea & Febiger: Philadelphia. 31-38.

Dyce, K.M., Sack, W.O., and Wensing, C.J.G. (1987) <u>Textbook of Veterinary Anatomy</u>. W.B. Saunders Company: Philadelphia. 554-562.

Dyson, S.J. (1991) "Lameness due to pain associated with the distal interphalangeal joint: 45 cases." *Equine vet. J.* 23, 128-135.

Dyson, S.J. (1994) "A comparison of responses to analgesia of the navicular bursa and intra-articular analgesia of the of the distal interphalangeal joint in 102 horses." In: International Symposium on Podotrochleosis. In-Verlag de Dertschen Reiberticher Vereinrgung, Warendorf. 152-164.

Dyson, S.J. and Kidd, L. (1993) "A comparison of responses to analgesia of the navicular bursa and intra-articular analgesia of the of the distal interphalangeal joint in 59 horses." *Equine vet. J.* 25, 93-98.

Edvinsson, L. and Uddman, R. (1993) <u>Vascular Innervation and Receptor Mechanisms</u>. Academic Press, Inc.: San Diego, CA. 252-258, 263.

Evans, W.F. (1976) <u>Anatomy and Physiology, Second Edition</u>. Prentice-Hall, Inc.: Englewood Cliffs, NJ. 51.

Getty, R. (1975) Sisson and Grossman's The Anatomy of the Domestic Animals, 5th ed., Chapter 15, edited by Getty, R. W.B. Saunders Company: Philadelphia. 291-296, 358-362.

Hale, A.R. and Burch, G.E. (1960) "The Arteriovenous Anastomoses and Blood Vessels of the Human Finger". Medicine 39, 191-240.

Herkenham, M. and Pert, C.B. (1982) "Light microscopic localization of brain opiate receptors: a general autoradiographic method which preserves tissue quality". J. Neuroscience 2, 1129-1149.

Hickman, J. (1989) "Navicular disease - what are we talking about?" Equine Vet. J. 21, 395-398.

Hood, D.M., Amoss, M.S., Hightower, D., McDonald, D.R., McGrath, J.P., McMullan, W.C., and Scrutchfield, W.L. (1978) "Equine laminitis: radioisotope analysis of the hemodynamics of the foot during acute laminitis." *J. Equine Med. Surgery* 2, 439-444.

Hoppner, D. and Piefschamanne, eds. (1994) "International symposium on podotroclosis" Verlag der Deutschen Reiterlichen Vereinigung, Warendorf, 1-291.

James, P.T., Kemler, A.G., and Smallwood, J.E. (1980) "The arterial supply to the distal sesamoid bones of the equine thoracic and pelvic limbs." J. of Veterinary Orthopedics 2 (1), 38.

Kimball, E.S. (1990) "Substance P, cytokines and arthritis." Ann. N.Y. Acad. Sci. 594, 293-308.

Kobluk, C.N., Ames, T.R., and Geor, R.J. (1995) <u>The Horse: Diseases & Clinical Management</u>. W.B. Saunders Company: Philadelphia. 678-682.

Konsgaard, E. (1982) "The muscle function in the forelimb of the horse: an electromyographical and kinesiological study." Thesis. Copenhagen, Denmark.

MacGregor, C.M. (1989) "Navicular disease - in search of definition." Equine Vet. J. 21 (6), 389-391.

Mankin, H.J. and Radin, E.L. (1997) "Structure and function of joints." <u>In: Arthritis and Allied Conditions</u>, 13th ed., edited by Koopman, W.J. Williams and Wilkins: Baltimore.

Mantyh, P., Catton, M.D., Boehmer, C.O., et al. (1989) "Receptors of sensory neuropeptides in human inflammatory disease: implications for the effector role of sensory neurons." *Peptides* 10, 627-645.

McLachlan, E.M. and Janig, W. (1983) "The cell bodies of origin of sympathetic and sensory axons in some skin and muscle nerves of the cat hindlimb". J. Comp. Neurol. 214, 115-130.

Meier, H.P. (1994) "A review of investigations of etiology of navicular disease." International Symposium on Podotroclosis. edited by Hertsch, B. FN-Verlag der Deutschen Reiterlichen Vereinigung: Munich. 57-59.

Molyneux, G.S., Haller, C.J., Mogg, K., and Pollitt, C.C. (1994) "The structure, innervation and location of arteriovenous anastomoses in the equine foot." *Equine vet. J.* 26, 305-312.

Molyneux, G.S. and Bryden, M.M. (1978) "Arteriovenous anastomoses in the skin of seals." Anat. Rec. 191, 239-252.

Nickel R., Schummer, A., Seiferle, E., Frewein, J., and Wille, K.H. (1979) <u>Locomotor</u> System of the Domestic Mammals, Volume 1. Springer-Verlag: New York. 198-201.

Ostblom, L., Lund, C., and Melsen, F. (1989a) "Histological study of navicular bone disease." *Equine vet. J.* 14: 199-202.

Ostblom, L., Lund, C., and Melsen, F. (1989b) "Navicular bone disease: a comparative histomorphometric study." *Equine Vet. J.*, 21 (6), 431-433.

Pool, R.R., Meagher, D.M., and Stover, S.M. (1989) "Pathophysiology of navicular syndrome." *Vet. Clinics of North America*, 5, 109-129.

Rijkenhuizen, A.B.M., Nemeth, F., Dik, K.J., and Goedegebuure, S.A. (1989a) "The arterial supply of the navicular bone in the normal horse." *Equine Vet. J.*, 21 (6), 399-404.

Rijkenhuizen, A.B.M., Nemeth, F., Dik, K.J., and Goedegebuure, S.A. (1989b) "The arterial supply of the navicular bone in adult horses with navicular disease." *Equine Vet.* J., 21 (6), 418-424.

Rijkenhuizen, A.B.M., Nemeth, F., Dik, K.J., and Goedegebuure, S.A. (1989c) "Development of the navicular bone in foetal and young horses, including the arterial supply." *Equine Vet. J.*, 21 (6), 405-412.

Rijkenhuizen, A.B.M., Nemeth, F., Dik, K.J., and Goedegebuure, S.A. (1989d) "The effect of unilateral resection of segments of both palmar digital arteries on the navicular bone in ponies: an experimental study." *Equine Vet. J.*, 21 (6), 413-417.

Rijkenhuizen, A.B.M., Nemeth, F., Dik, K.J., and Goedegebuure, S.A. (1989e) "The effect of artificial occlusion of the ramus navicularis and its branching arteries on the navicular bone in horses: an experimental study." *Equine Vet. J.*, 21 (6), 425-430.

Rooney, J.R., (1969) <u>Biomechanics of Lameness in Horses</u>. Williams and Wilkens Company: Baltimore. 77, 180-184.

Sack, W.O., (1991) Rooney's Guide to the Dissection of the Horse, 6th ed. Veterinary Textbooks: Ithaca, NY. 169-177.

Schryver, H.F., Bartel, D.L., Langrana, N., and Lowe, J.E. (1978) "Locomotion in the horse: kinematics and external and internal forces in the normal equine digit in the walk and trot." *Am. J. Vet. Res.* 39, 1728-1733.

Schummer, A., Wilkens, H., Vollmerhaus, B., Habermehl, K.-H. (1981) <u>The Anatomy of the Domestic Animals</u> Volume 3: The Circulatory System, the Skin, and the Cutaneous Organs of the Domestic Mammals. Springer-Verlag: New York. 552-557.

Sisson, S. (1975) "Equine syndesmology." In <u>Sisson and Grossman's The Anatomy of the Domestic Animals, 5th ed.</u>, Chapter 16, edited by Getty, R. W.B. Saunders Company: Philadelphia. 349-375.

Slauson, D.O., and Cooper, B.J. (1990) <u>A Textbook of Comparative General Pathology</u>, <u>2nd ed.</u>, Williams and Wilkins: Baltimore. 246-260.

Sonea, I.M. (1993) <u>Sensory Innervation of the Equine Lung: Distribution of Nerve Fibers and Tachykinin Receptors</u>. PhD Dissertation submitted to Michigan State University.

Stashak, T.S. (1987) Adams' Lameness in Horses, 4th ed., Lea & Febiger: Philadelphia. 499-514.

Taylor, D.C.M. and Dierau, F.K. (1991) <u>Nociceptor Afferent Neurons</u>. Manchester University Press, Manchester. 3-14.

Thomas, C.L. (1989) <u>Taber's Cyclopedic Medical Dictionary</u>, F.A. Davis Company: Philadelphia. 1645.

Turner, T. (1989) "Diagnosis and treatment of navicular syndrome in horses." Vet. Clin. N. Am.: Equine Pract. 5, 131-144.

Turner, T. (1991) "Navicular disease." In <u>Equine Medicine and Surgery, 4th ed.</u>, edited by Colohan, P., Mayhew, IlG., Merritt, A., and Moore, J. American Veterinary Publications: Goleta. 1346-1350.

Turner, T. (1996) "Role of hoof imbalance on navicular disease." *Pierdeheilkunde*, 41-48.

Van Wulfen, K.K. and Bowker, R.M. (1997) "The Intersection of the DSIL and the DDFT and its Relationship to Navicular Syndrome". AAEP Proceedings, 43.

Weihe, E. (1990) "Neuropeptides in primary afferent neurons". <u>The Primary Afferent Neuron</u>. W. Zenker and W.L. Neuhber. Plenum Press, New York. 127-159.

Wintzer, H.J. and Schlarman, B. (1971) "Aur Arteriellen Blutuersorgung des Strahlbein und der B Luchbeine." *Pferd. Zbl. Vet. Med. Ass.*, 18, 644.

Zimny, M.L., St. Onge, M., and Schutte, M. (1985) "A modified gold chloride method for the demonstration of nerve endings in frozen sections." *Stain Technology*, 60 (5), 305-306.

**PUBLICATIONS** 

#### **PUBLICATIONS**

Bowker, R.M., Van Wulfen, K.K., and Grentz, D.J. (1995) "Nonselectivity of Local Anesthetics Injected into the Distal Interphalangeal Joint and the Navicular Bursa". AAEP Proceedings, Vol. 41, 240-242.

Bowker, R.M. and Van Wulfen, K.K. (1996) "Microanatomy of the intersection of the distal sesamoidean impar ligament and the deep digital flexor tendon: A preliminary report". Pferdeheilkunde 12, 4, 623-627.

Bowker, R.M., Van Wulfen, K.K., and Springer, S. (1997) "Macroscopic and Microscopic Anatomy of the Ungual Cartilage: A Hemodynamic Flow Hypothesis of Energy Dissipation". AAEP Proceedings, Vol. 43, 354-355.

Bowker, R.M., Linder, K., Van Wulfen, K.K., and Sonea, I.M. (1997) "Anatomy of the distal interphalangeal joint of the mature horse: relationships with navicular suspensory ligaments, sensory nerves and neurovascular bundle". Equine vet. J. 29, 26-135.

Bowker, R.M., Van Wulfen, K.K., Springer, S.E., Linder, K.E. (1998) "Functional anatomy of the cartilage of the distal phalanx and digital cushion in the equine foot and a hemodynamic flow hypothesis of energy dissipation." American J. of Veterinary Research, Vol. 59, No. 8, 961-968.

Van Wulfen, K.K. and Bowker, R.M. (1997) "Intersection of the DSIL and the DDFT and its Relationship to Navicular Syndrome". AAEP Proceedings, Vol. 43, 405-406.

MICHIGAN STATE UNIV. LIBRARIES
31293020509976